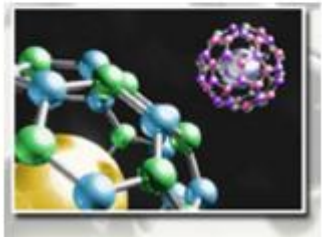




**PHYSICS and
ASTROPHYSICS**



**CHEMICAL and
MATERIAL SCIENCES**

Ion Beam Based Techniques for Materials Science

Teachers:

Paolo Olivero, Ettore Vittone

Physics Department, University of Torino

www.solid.unito.it

2 CFU : 8 h

Tuesday 2.5.2017, h. 16-18, Aula Verde, Physics Dept. - Ettore Vittone

Wednesday 3.5.2017, h. 16-18, Aula Wick, Physics Dept. - Ettore Vittone

Thursday 4.5.2017, h. 16-18, Aula D, Physics Dept. - Paolo Olivero

Friday 5.5.2017, h. 16-18, Aula Verde, Physics Dept. - Paolo Olivero

CAMPUSNET WEB SITE:

http://dott-scm.campusnet.unito.it/do/corsi.pl/Show?_id=j56m

Final exam:

Brief seminar (15 min) on a topic relevant to Ion Beam Based Techniques

Introduction

Instrumentation

Accelerators

Ion sources

Detectors

Ion-Solid interaction

Electronic energy loss

Nuclear energy loss

IBA techniques

RBS

Sample (Ion,Ion) Sample

Structural/elemental analysis

ERDA

Sample (Ion,Ion') Sample

PIXE

Sample(Ion, x ray) Sample

Structural analysis

IBIC

Sample(Ion, electron-hole) Sample

Functional analysis

IBA

Instrumentation

Accelerators

Ion sources

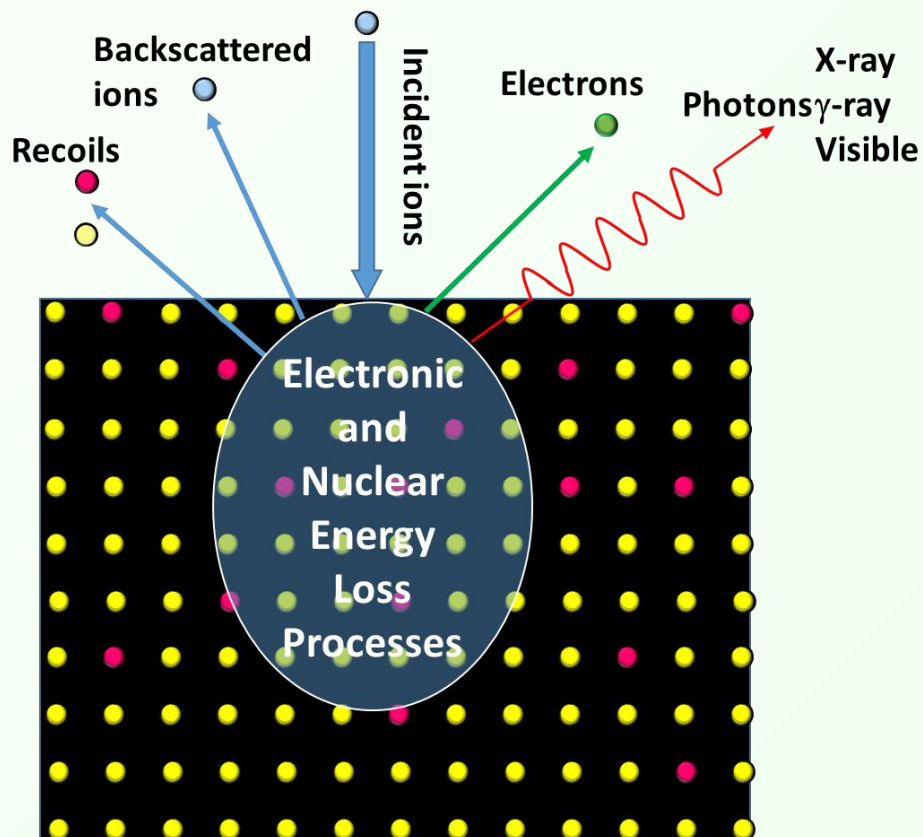
Detectors

Ion-Solid
interaction

Electronic energy loss

Nuclear energy loss

IBA techniques



Compositional analysis

Structural analysis

Functional analysis

IBA

Instrumentation

Accelerators

Ion sources

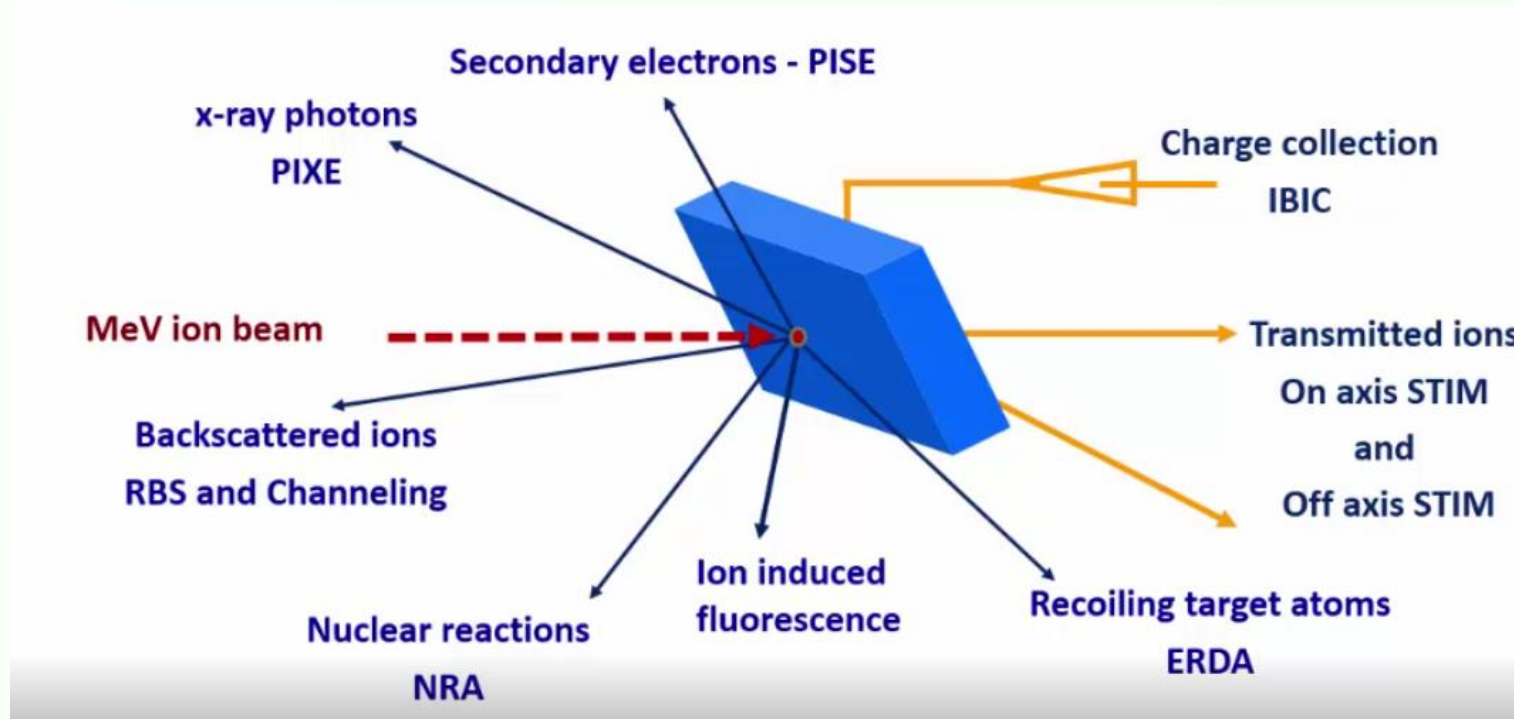
Detectors

Ion-Solid
interaction

Electronic energy loss

Nuclear energy loss

IBA techniques



Compositional analysis

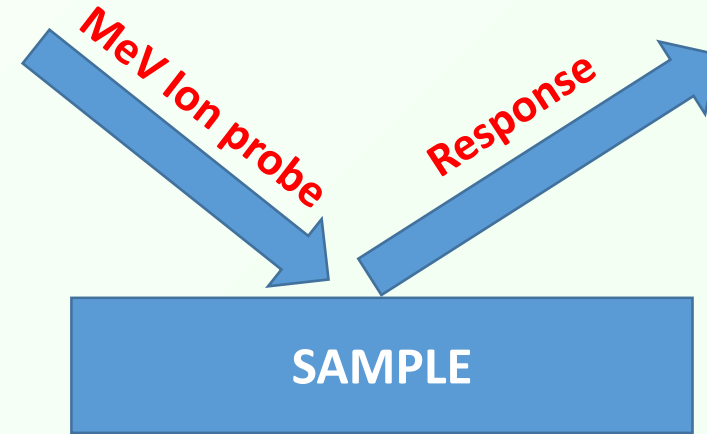
Structural analysis

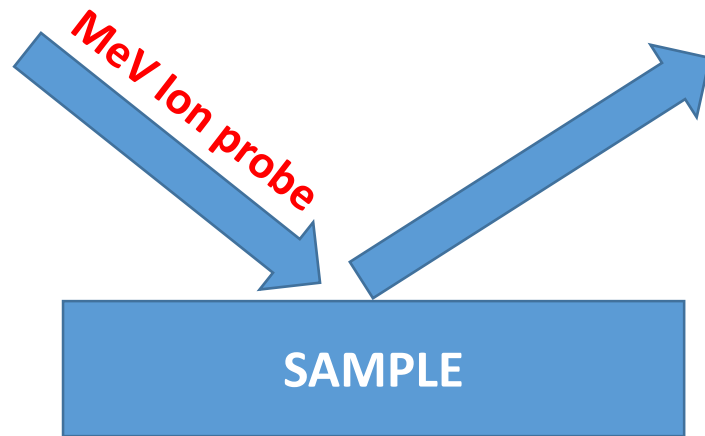
Functional analysis

Main Features

- ✓ Quantitative multi-elemental analysis
- ✓ High sensitivity (1-100 ppm in at/cm³)
- ✓ Depth profiling (1-10⁴ nm)
- ✓ No invasive analysis
- ✓ No sample preparation
- ✓ Micro-spectroscopy (resolution μm)

- ✓ Compositional analysis
- ✓ Structural analysis
- ✓ Functional analysis (electronic devices)

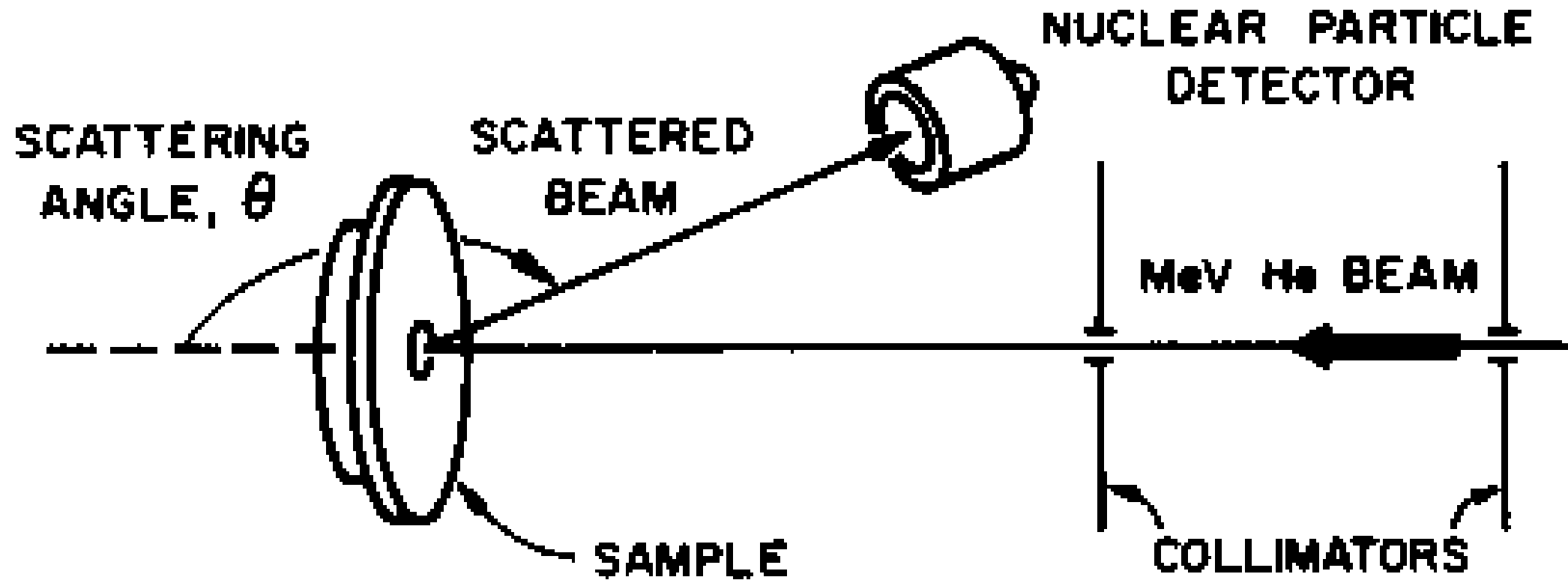




Rutherford Backscattering Spectrometry (RBS)

- ❑ RBS is an ion scattering technique that is used for the surface layer analysis of solids.
- ❑ A target is bombarded with ions at an energy in the MeV-range (0.5 – 4 MeV)
- ❑ The energy of the backscattered projectiles is recorded with an energy sensitive detector, typically a solid state detector.
- ❑ RBS allows the quantitative determination of the composition of a material and depth profiling of individual elements.

- ❑ quantitative without the need for reference samples,
- ❑ nondestructive,
- ❑ has a good depth resolution of the order of several nm,
- ❑ and a very good sensitivity for heavy elements of the order of parts-per-million (ppm).



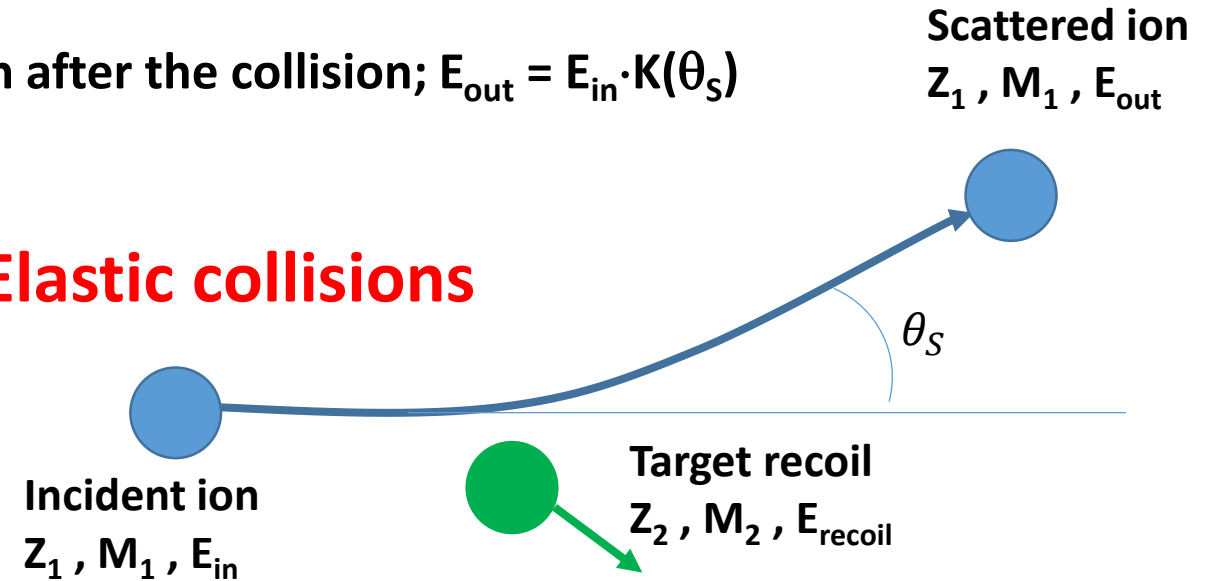
Fraction of the ion energy which remains with the ion after the collision; $E_{out} = E_{in} \cdot K(\theta_s)$

Kinematic factor $K(\theta_s)$; θ_s scattering angle.

Energy of the recoil nucleus: $E_{recoil} = (1 - K(\theta_s)) \cdot E_{in}$

TARGET MASS DISCRIMINATION

Elastic collisions

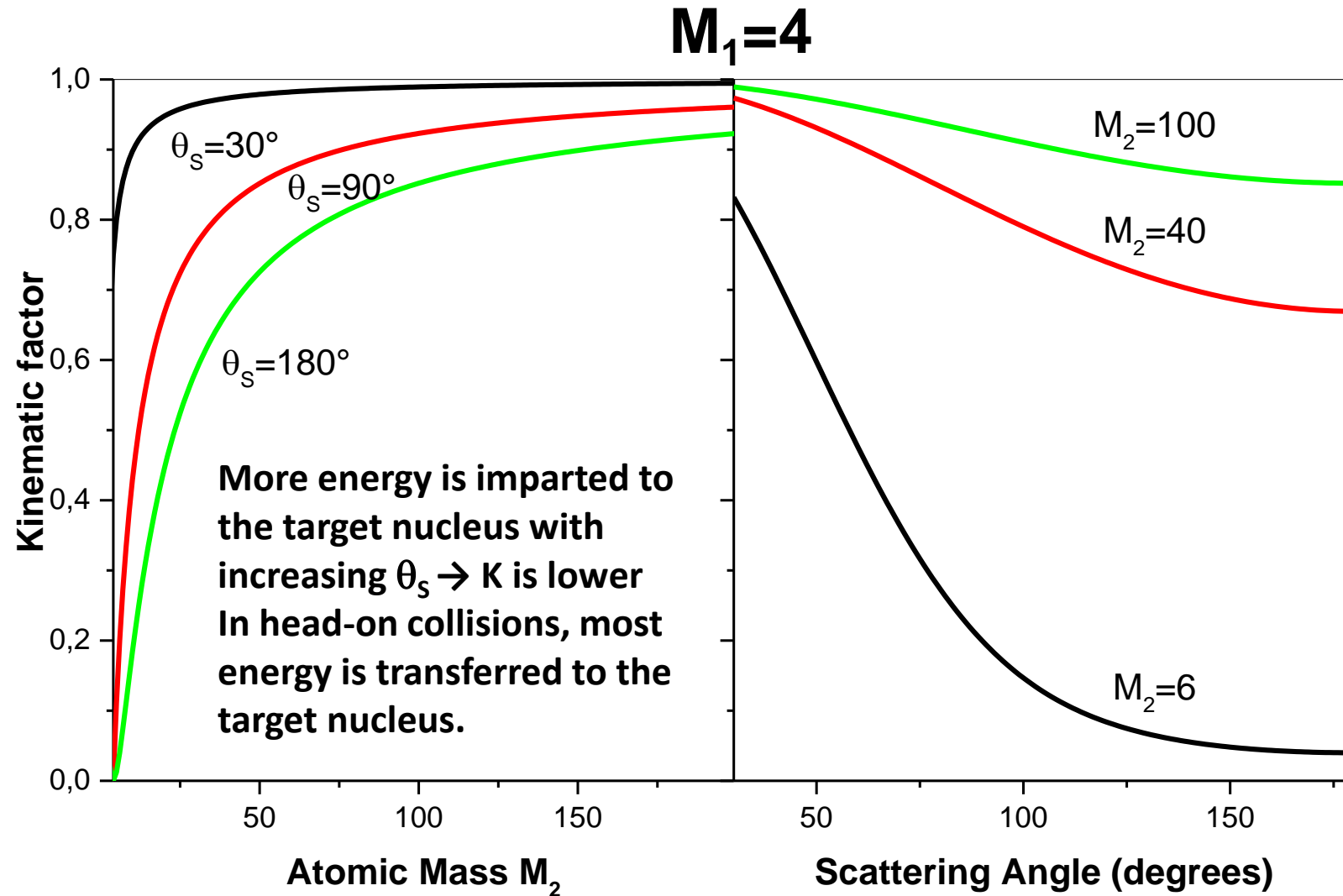


From the conservation of energy and momentum, in non-relativistic form and in the laboratory reference frame:

$$K(\theta_s) = \frac{E_{out}}{E_{in}} = \left\{ \frac{\sqrt{1 - \left(\frac{M_1}{M_2}\right)^2 \cdot \sin^2(\theta_s)} + \left(\frac{M_1}{M_2}\right) \cdot \cos(\theta_s)}{1 + \frac{M_1}{M_2}} \right\}^2$$

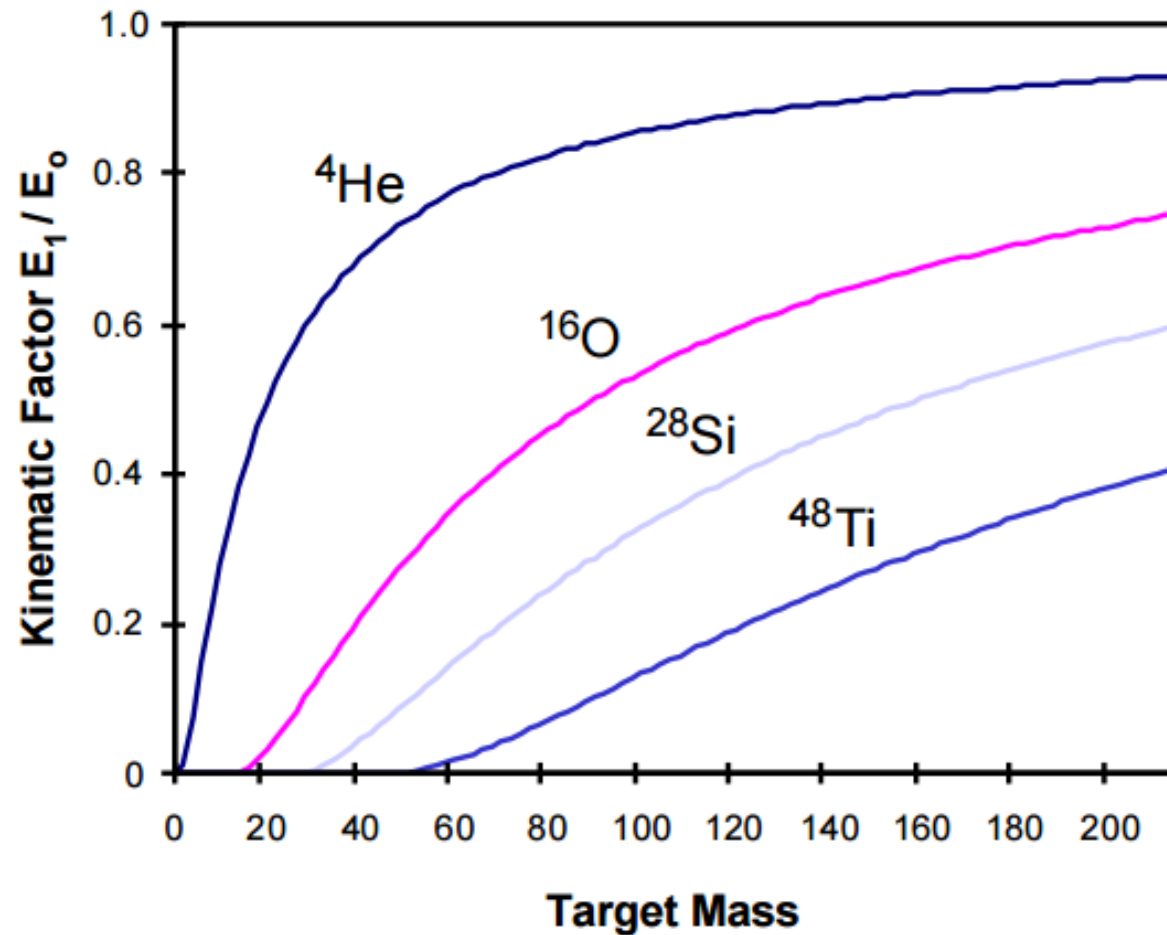
$K(\theta_s)$ depends only on the scattering angle and the ratio of masses of the ion and the atomic nucleus.

It does not depend on the ion energy



TARGET MASS DISCRIMINATION

$$\theta_s = 180^\circ$$

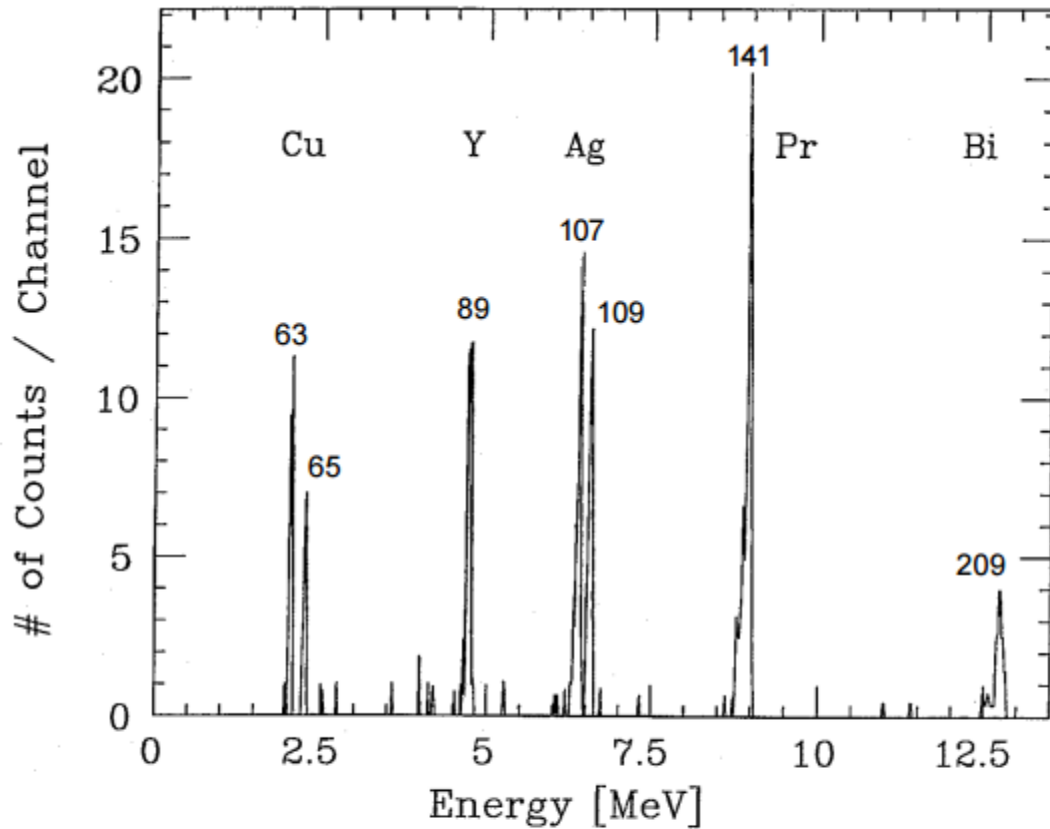


Kinematic factor as a function of **Target Mass** for a number of projectile types

TARGET MASS DISCRIMINATION

The signal from an atom at the sample surface will appear in the energy spectrum at a position $E_{\text{out}} = K \cdot E_{\text{in}}$

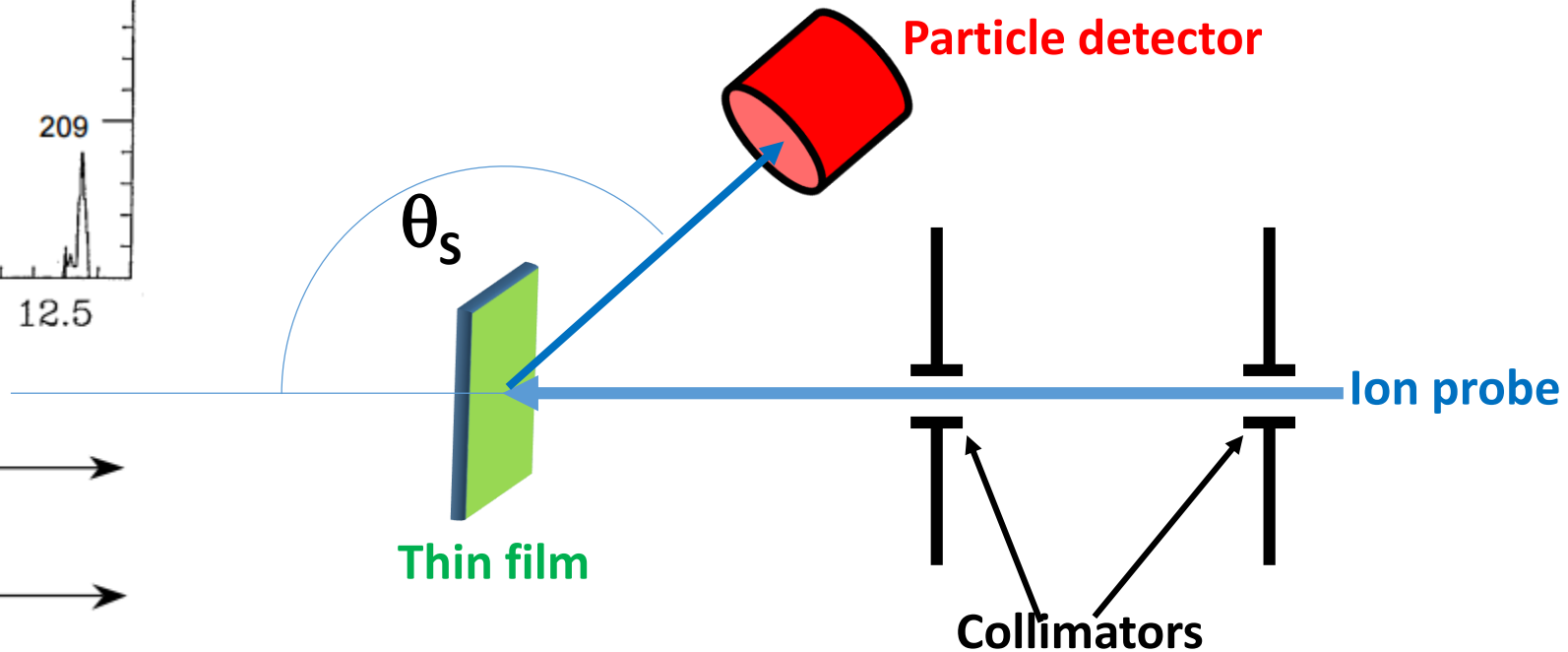
TARGET MASS DISCRIMINATION



Ion probe: ^{35}Cl

Target: **thin layer** of Cu, Y, Ag, Pr, Bi

Isotopes of Cu and Ag are resolved



kinematic factor

mass scale!

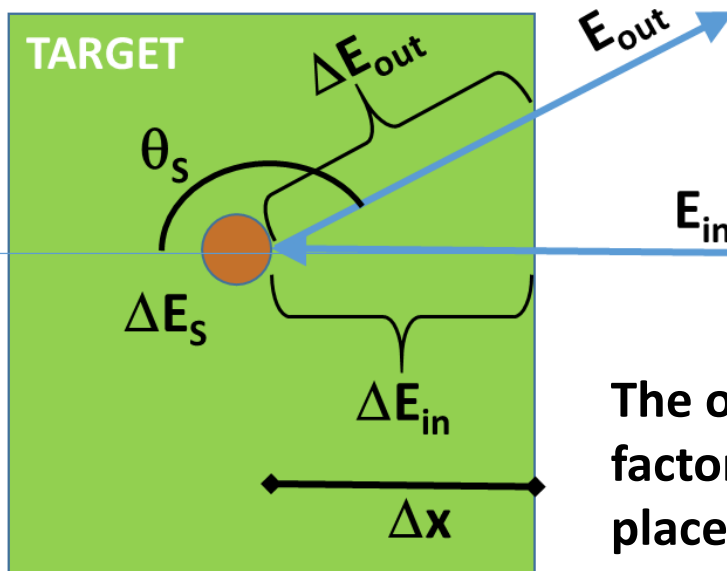
The signal from atoms of the same mass below the sample surface will be shifted by the amount of energy lost while the projectiles pass through the sample, both before ΔE_{in} and after ΔE_{out} collision

$$\text{Entry ion energy} = E_{in}$$

$$\text{Energy loss before scattering} = \Delta E_{in} = \left(\frac{dE}{dx} \right)_{in} \cdot \Delta x \quad \Rightarrow \quad \text{Energy before scattering} = E_x = E_{in} - \left(\frac{dE}{dx} \right) \cdot \Delta x$$

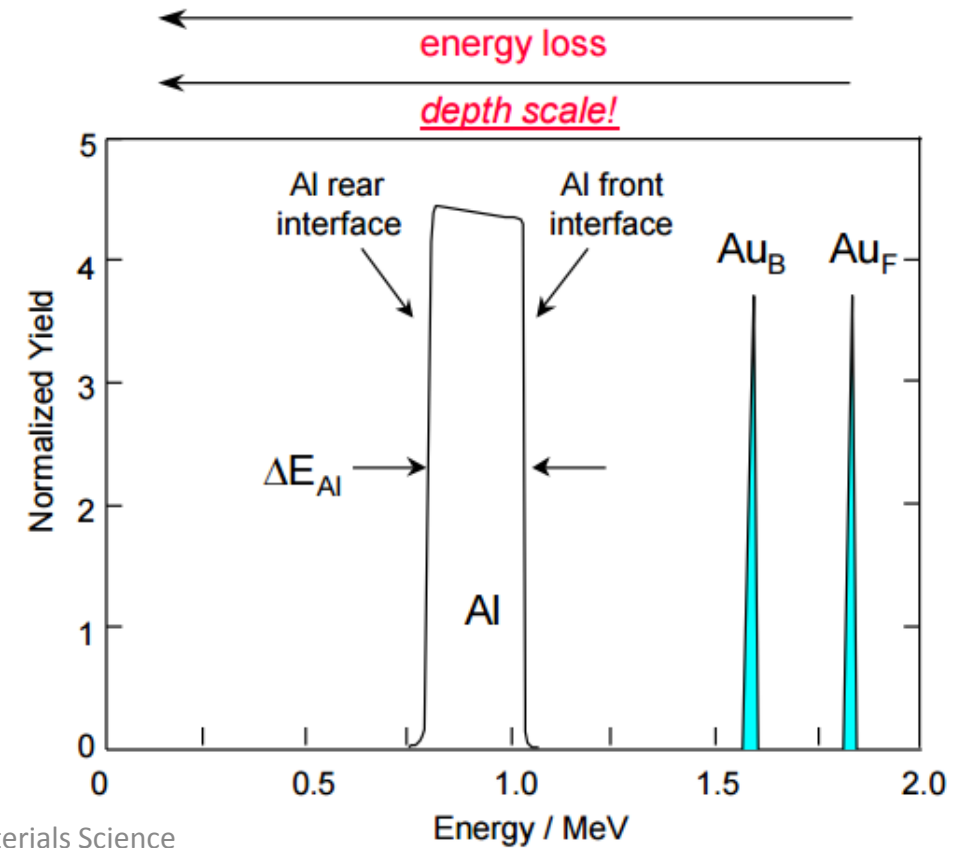
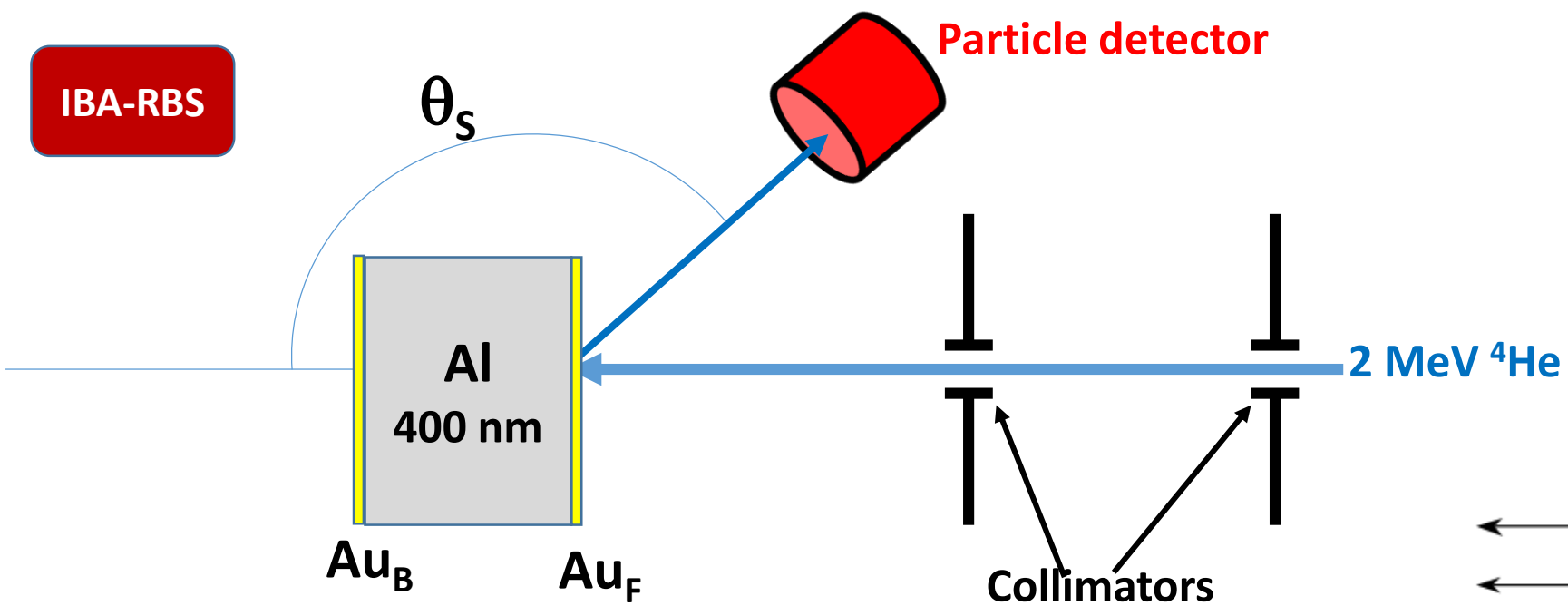
$$\text{Kinematic loss} = \Delta E_s = (1 - K) \cdot E_x \quad \Rightarrow \quad \text{Energy after scattering} = K \cdot E_x$$

$$\text{Energy loss after scattering} = E_{out} = \left(\frac{dE}{dx} \right)_{out} \cdot \frac{\Delta x}{\cos(\vartheta_s)} \quad \Rightarrow \quad \text{Output energy} = E_{out} = K \cdot E_x - \left(\frac{dE}{dx} \right)_s \cdot \frac{\Delta x}{\cos(\vartheta_s)}$$



$$E_{out} = K \cdot E_{in} - \left[K \cdot \left(\frac{dE}{dx} \right) + \frac{\left(\frac{dE}{dx} \right)_s}{\cos(\vartheta_s)} \right] \cdot \Delta x$$

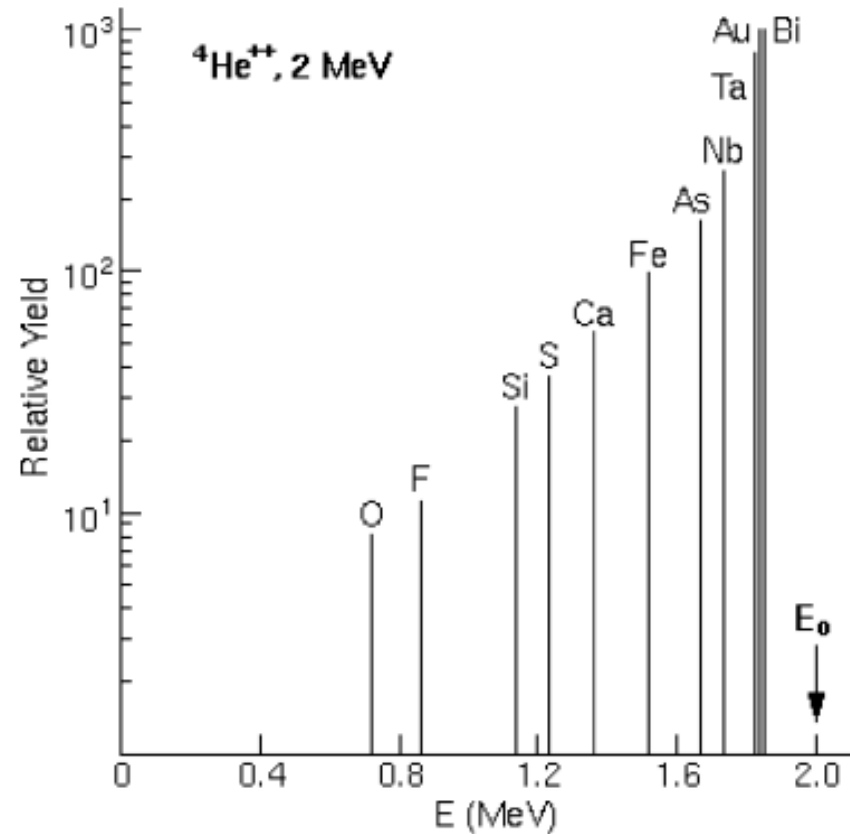
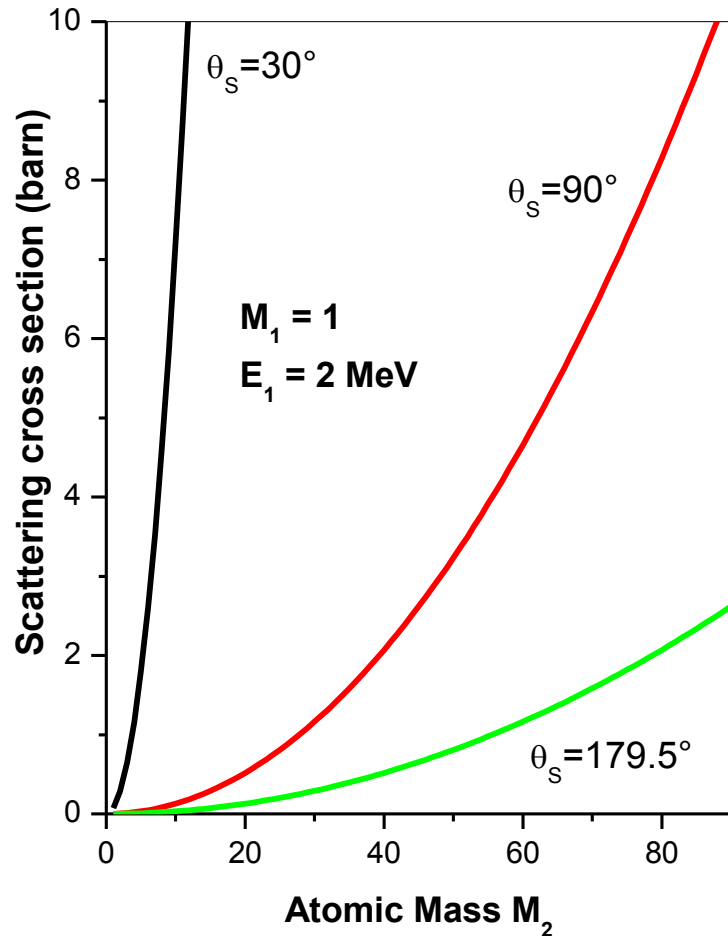
The output energy depends on the nuclear scattering through the kinematic factor K (Mass Discrimination) and on the depth at which the scattering took place (Depth Profile).



Scattering cross section

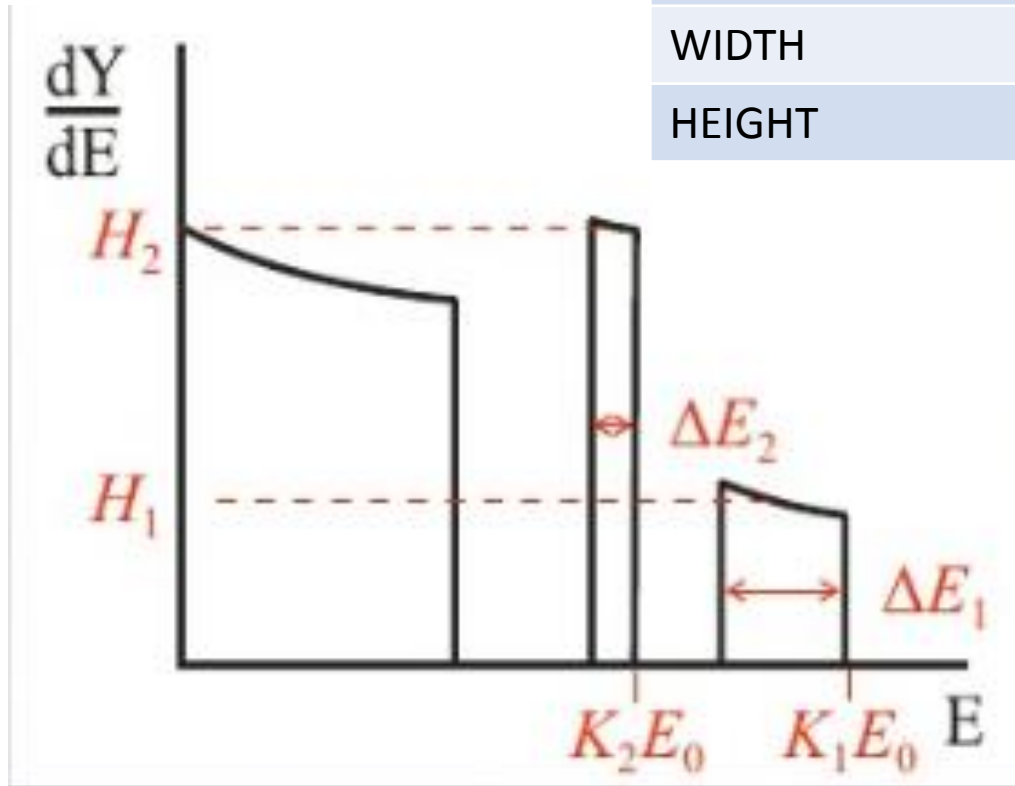
The yield of scattered particle is calculated using the differential scattering cross section which is given by Rutherford's formula:

$$\sigma(\theta_s) = \left[\frac{e^2}{4 \cdot \epsilon_0} \cdot \frac{Z_1 \cdot Z_2}{4 \cdot E_{in}} \right]^2 \cdot \left\{ \frac{1}{\sin^4 \left(\frac{\theta_s}{2} \right)} - 2 \left(\frac{M_1}{M_2} \right)^2 \right\}$$



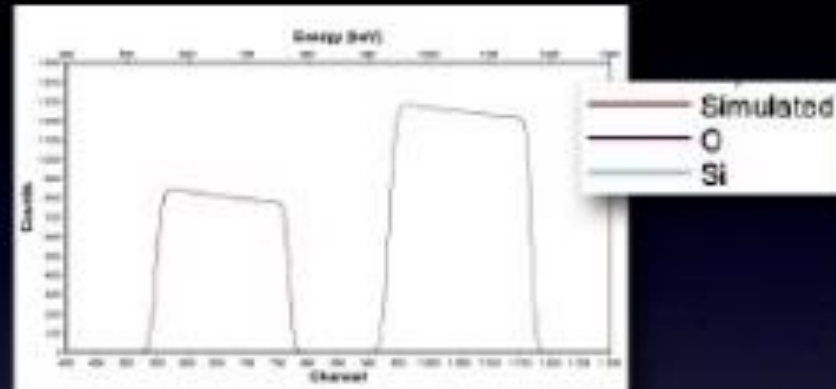
Scattering Yield as a function of the target atomic number

SEGNALE	INFORMAZIONE	
POSITION	MASS	Kinematic factor
WIDTH	THICKNESS/DEPTH	Stopping Power
HEIGHT	QUANTITY	Cross Section

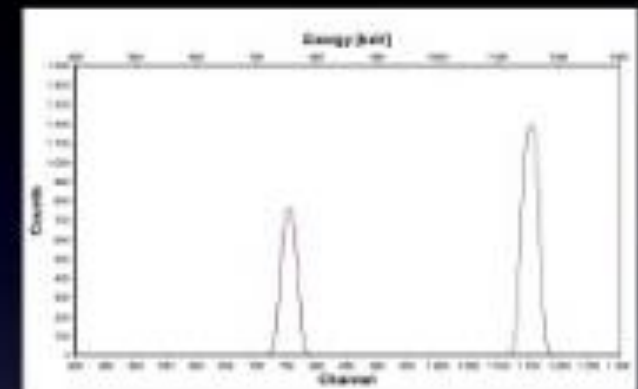


www.slideshare.net/max0068/chiarilezione-su-rutherford-backscattering-spectrometry-rsb-2012

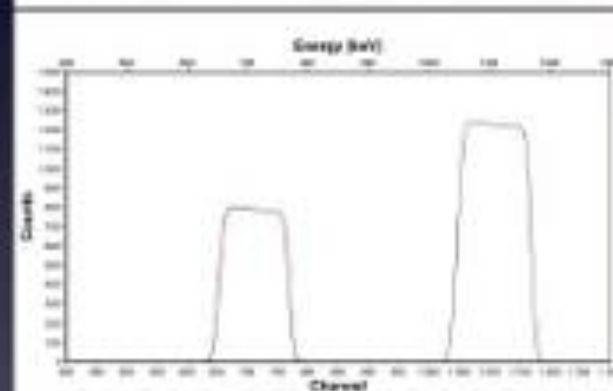
425 nm



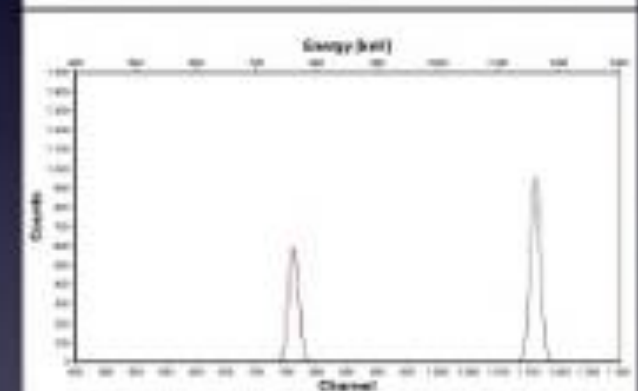
60 nm



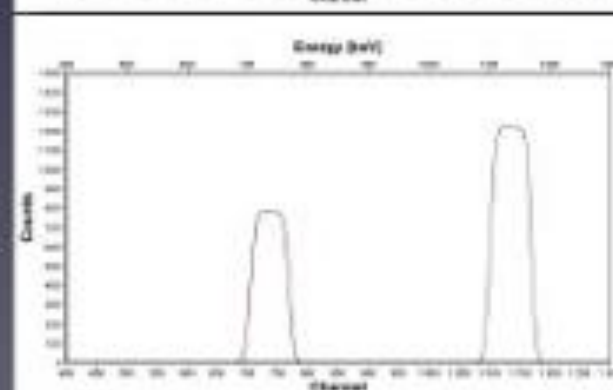
225 nm



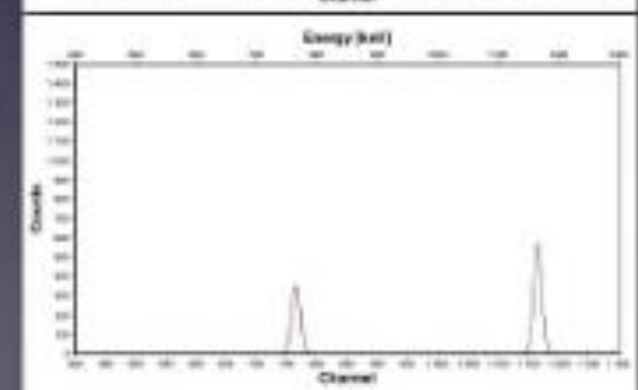
30 nm



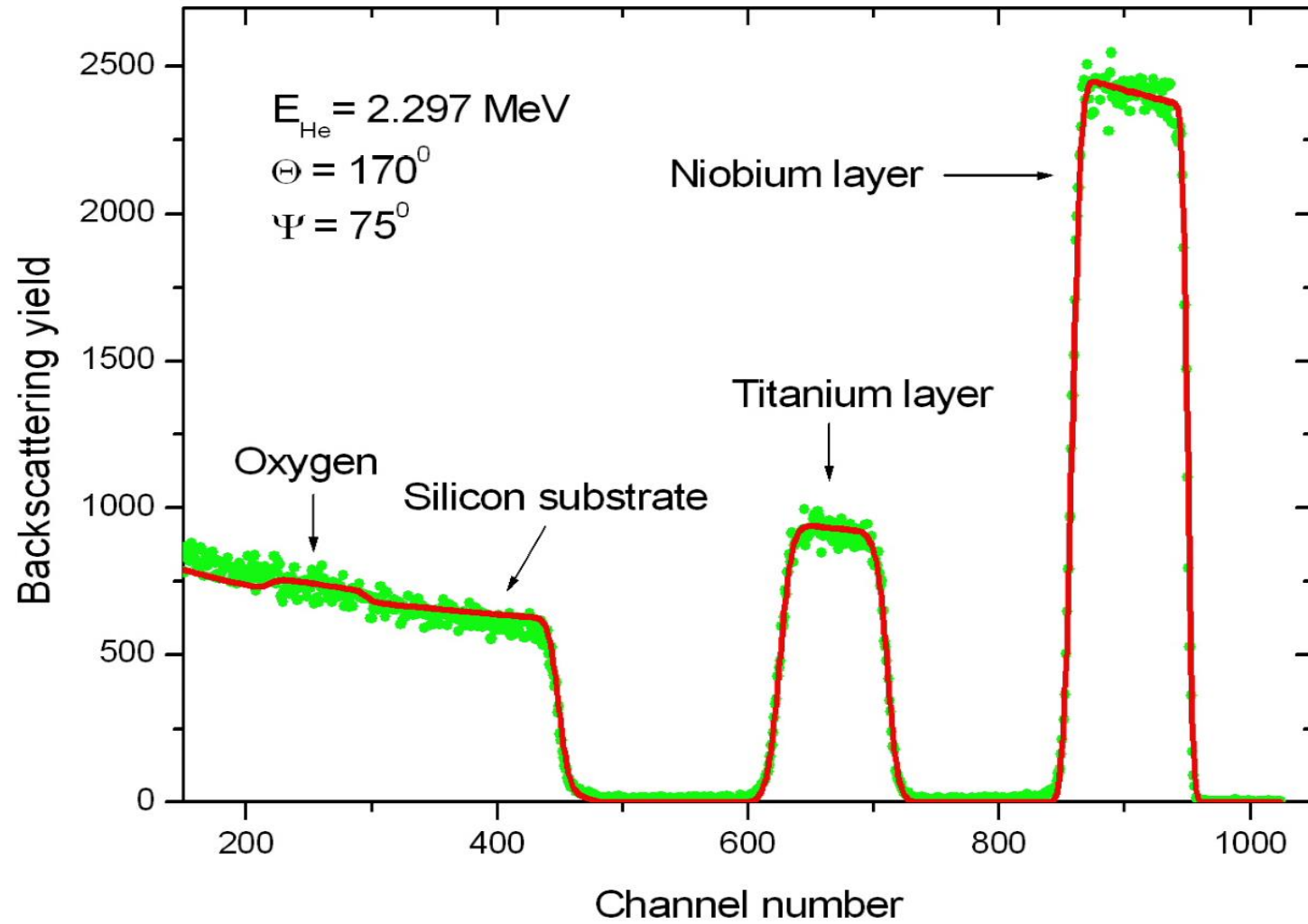
125 nm

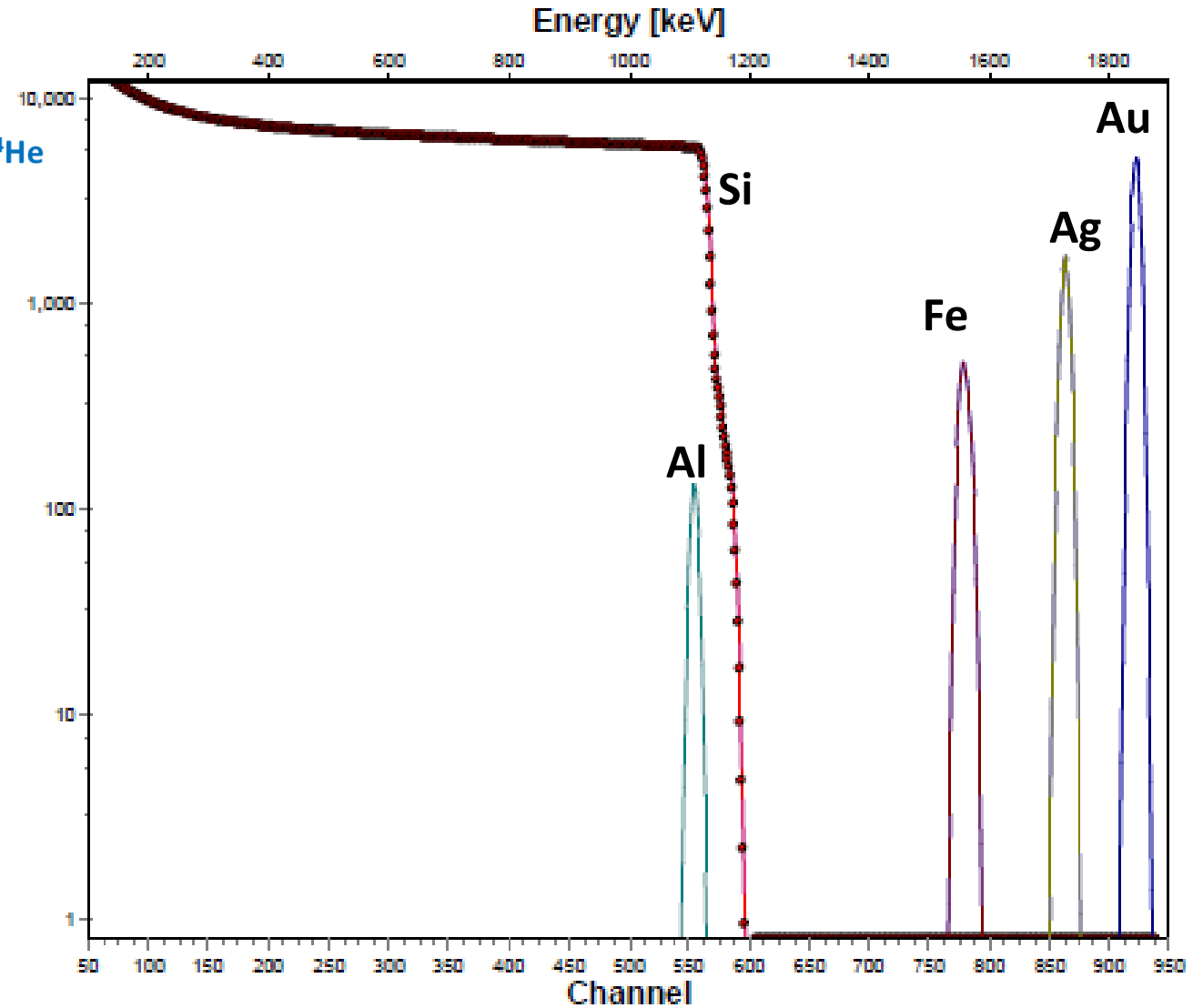
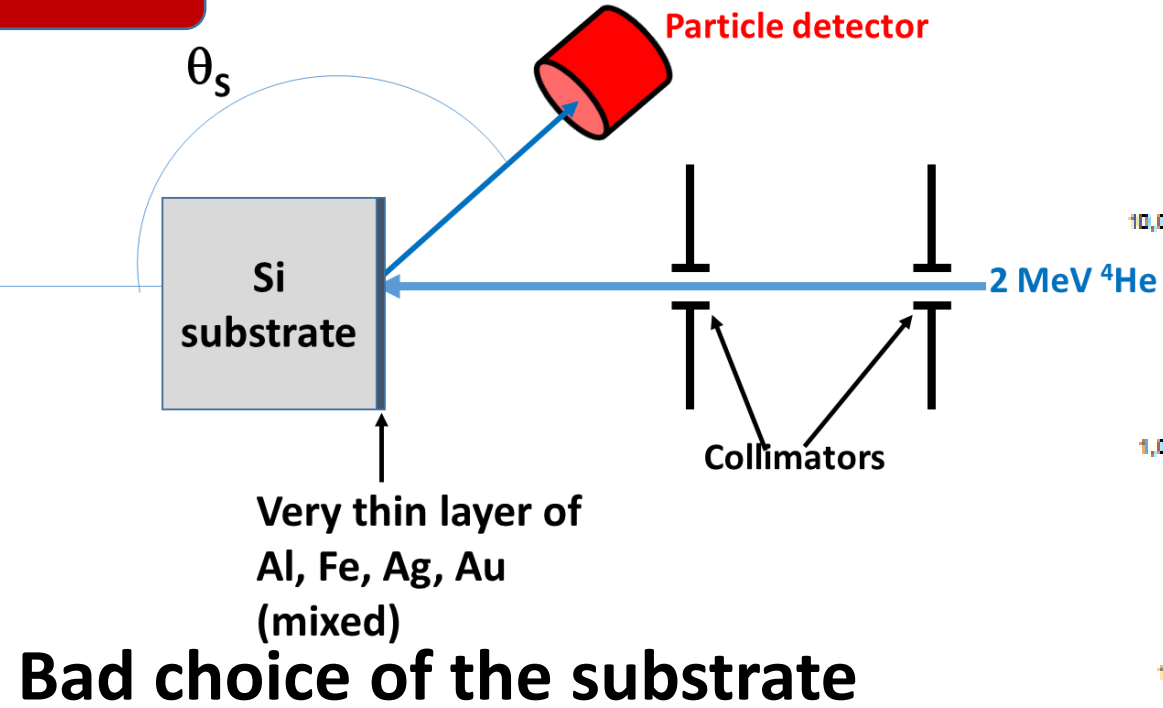


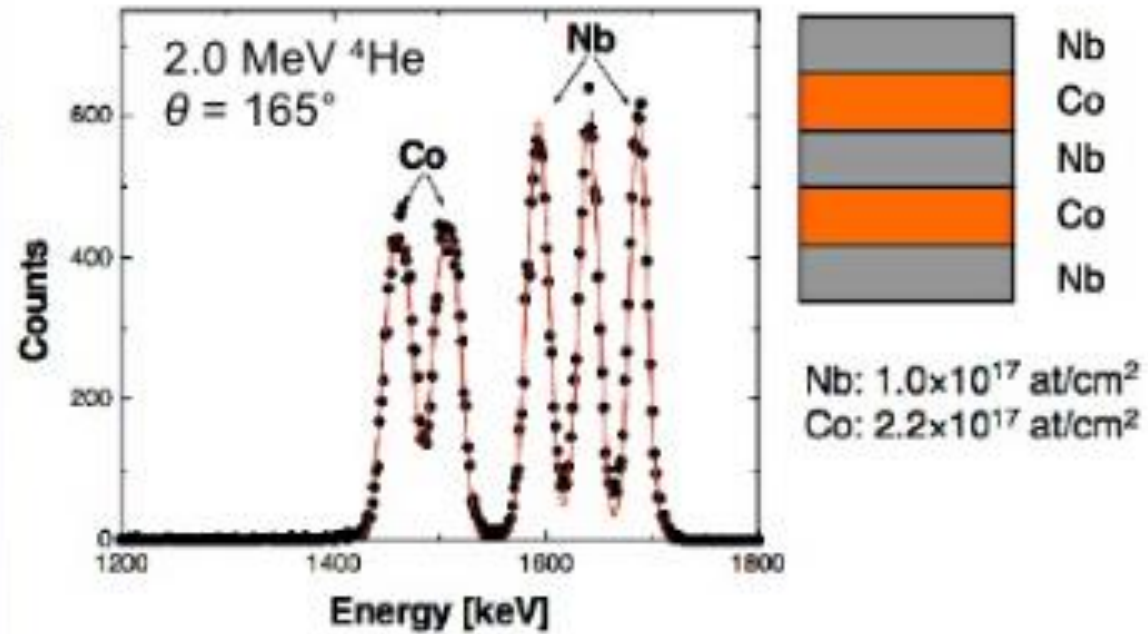
15 nm



Spettri simulati di un campione di SiO_2 bombardato con particelle α da 2 MeV, $\theta = 150^\circ$



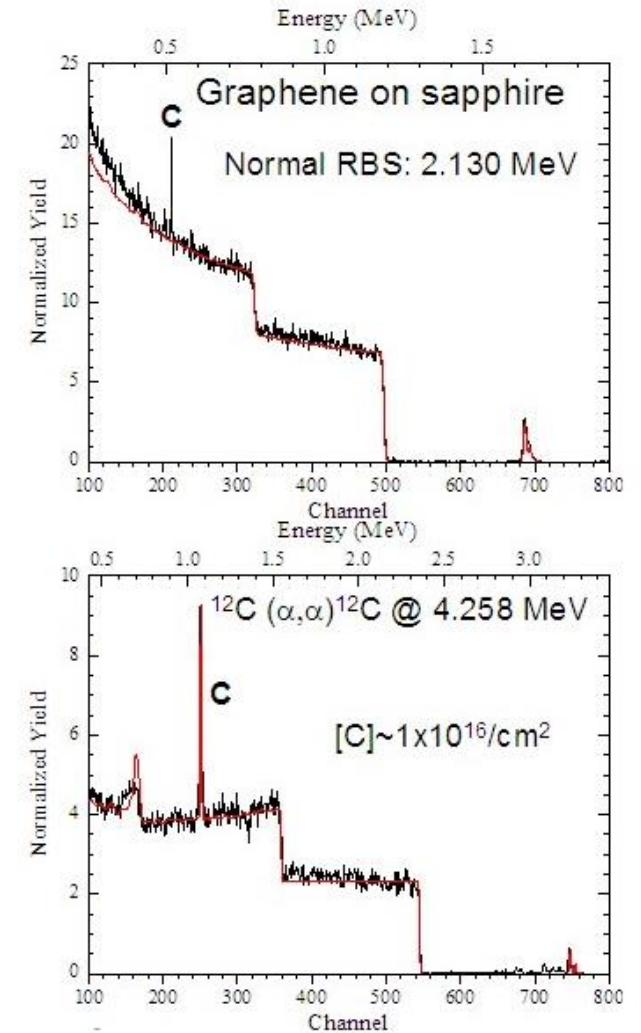
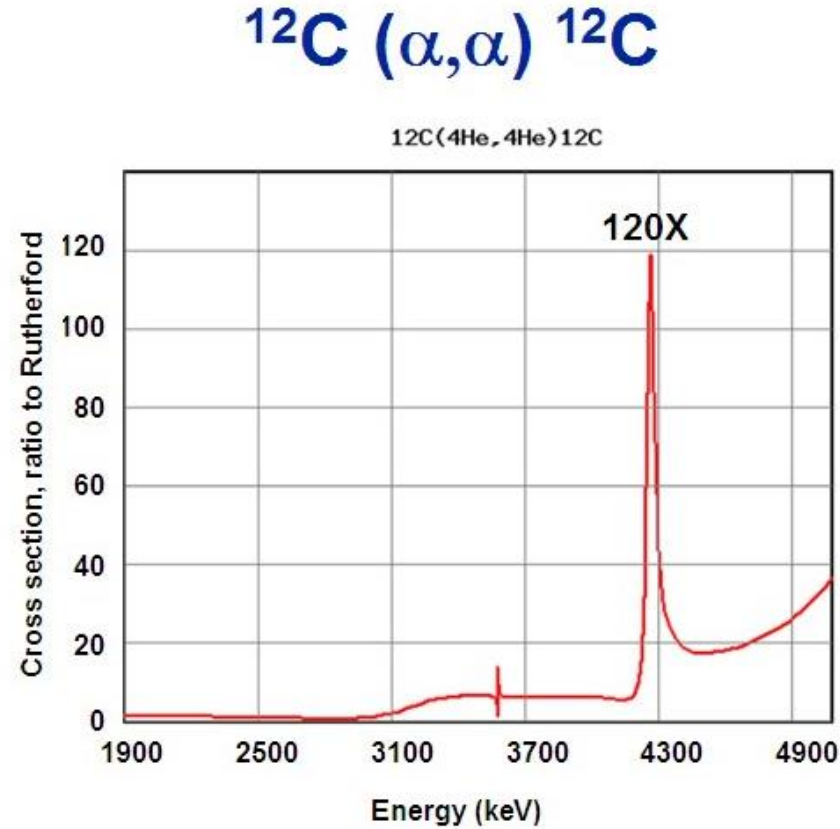




Non Rutherford Cross Section

When the collision diameter is very small and becomes comparable to the sum of the nuclear radii of the projectile and the target atom, the finite sizes of the nuclei and the nuclear force interactions lead to **deviations from the Rutherford scattering cross section**.

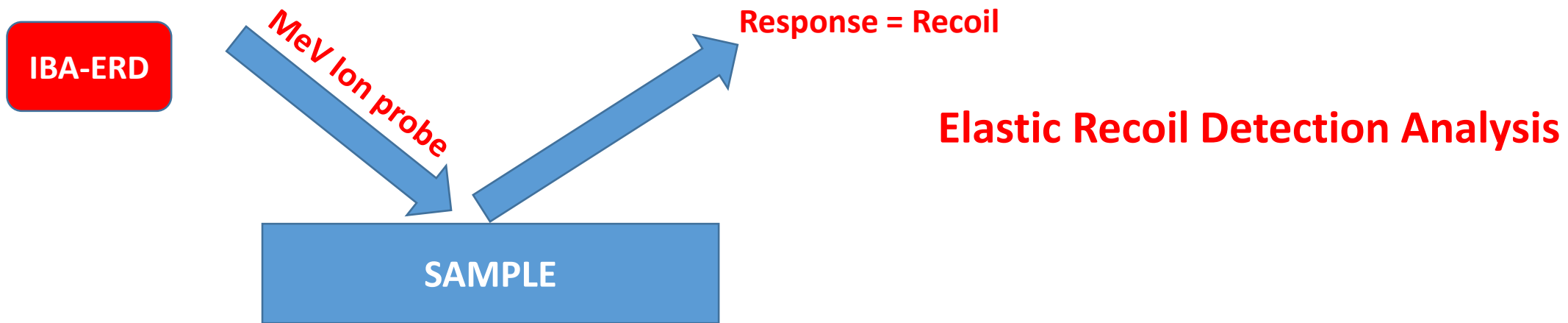
For MeV ion beams, this phenomenon can be observed in low Z projectile/target system where the Coulomb barrier is small.



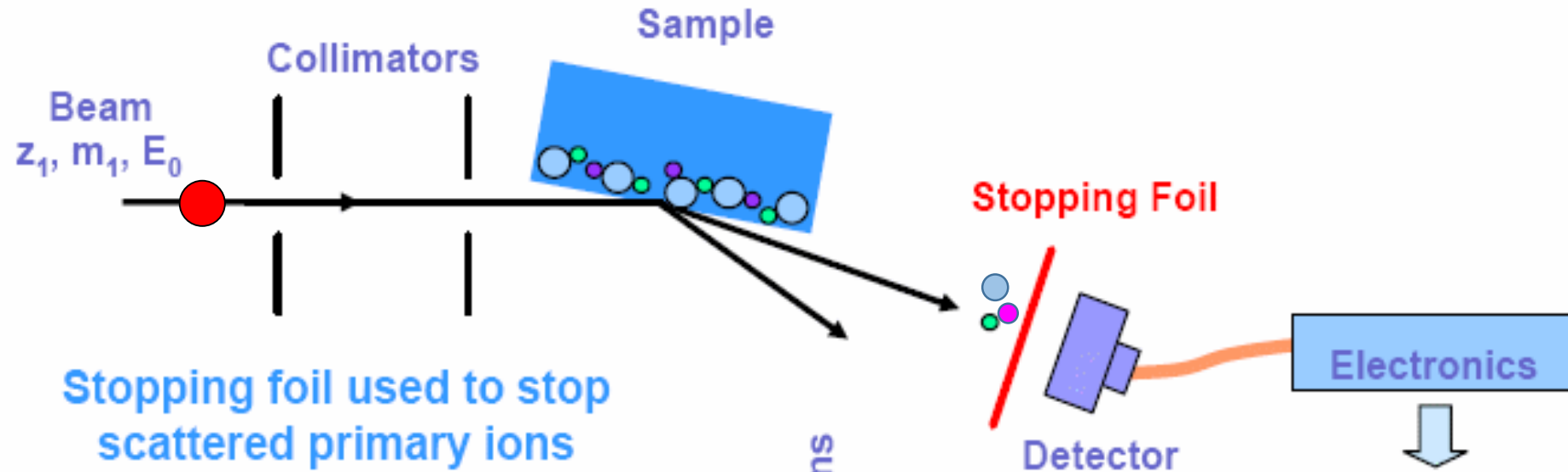
Main features of RBS

Elements	Be - U
Standard Conditions	2 MeV ^4He beam Silicon detector 10 minutes per sample
Precision	Stoichiometry: < 1% relative Thickness: < 5%
Sensitivity	Bulk: % to 10^{-4} , depending on Z Surface: 1 to 10^{-4} Monolayers
Depth Resolution	1 to 10 nm
Data analysis	e.g. by RUMP software: http://www.genplot.com/
Remarks	Accessible depth range $\sim 1\mu\text{m}$ No light elements detectable on heavy substrates

<http://cas.web.cern.ch/cas/Pruhonice/PDF/Doebeli.pdf>



If **light elements in heavy substrates** or elements lighter than the incident beam particles have to be analysed (e.g. hydrogen profiling) the **recoiling target atoms** can be detected in a grazing angle geometry

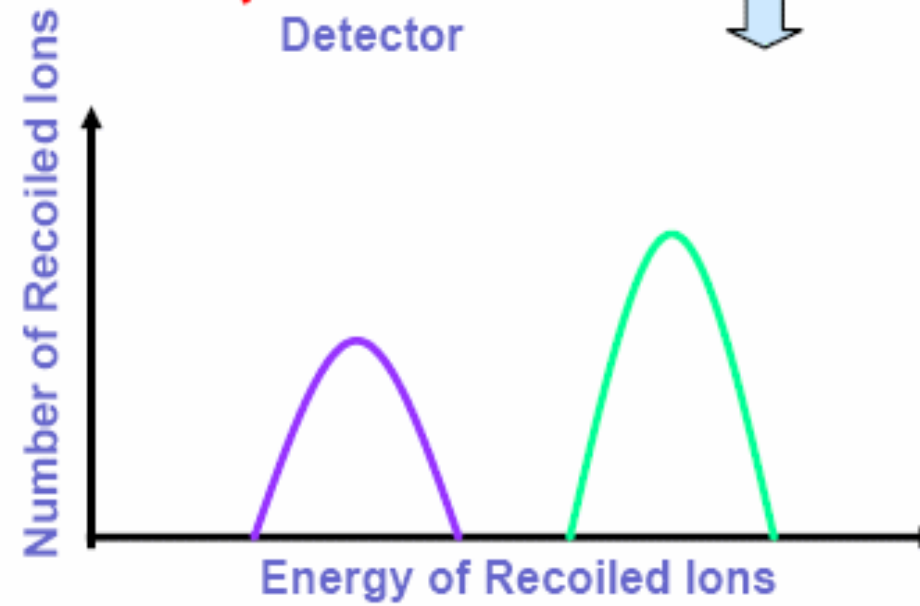


Stopping foil used to stop scattered primary ions

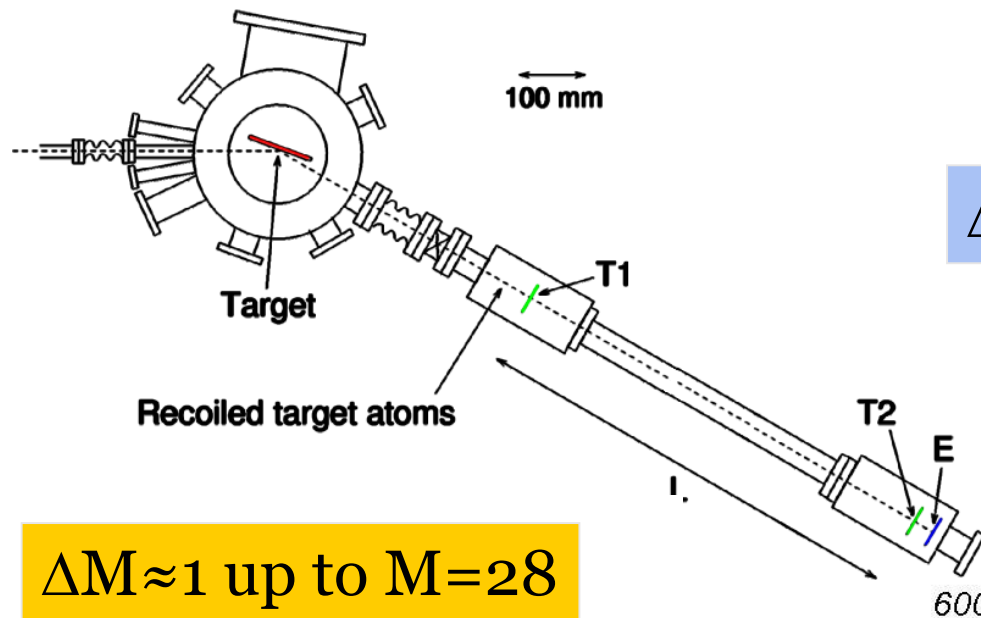
Detect recoils with mass less than that of the incident projectile ions

$$K' = \frac{4M_1M_2 \cos^2 \phi}{(M_1 + M_2)^2}$$

$$\left(\frac{d\sigma}{d\Omega}\right)_\phi = \left(\frac{Z_1Z_2e^2}{2E_0}\right)^2 \left(\frac{M_1}{M_2} + 1\right)^2 \frac{1}{\cos^3 \phi}$$



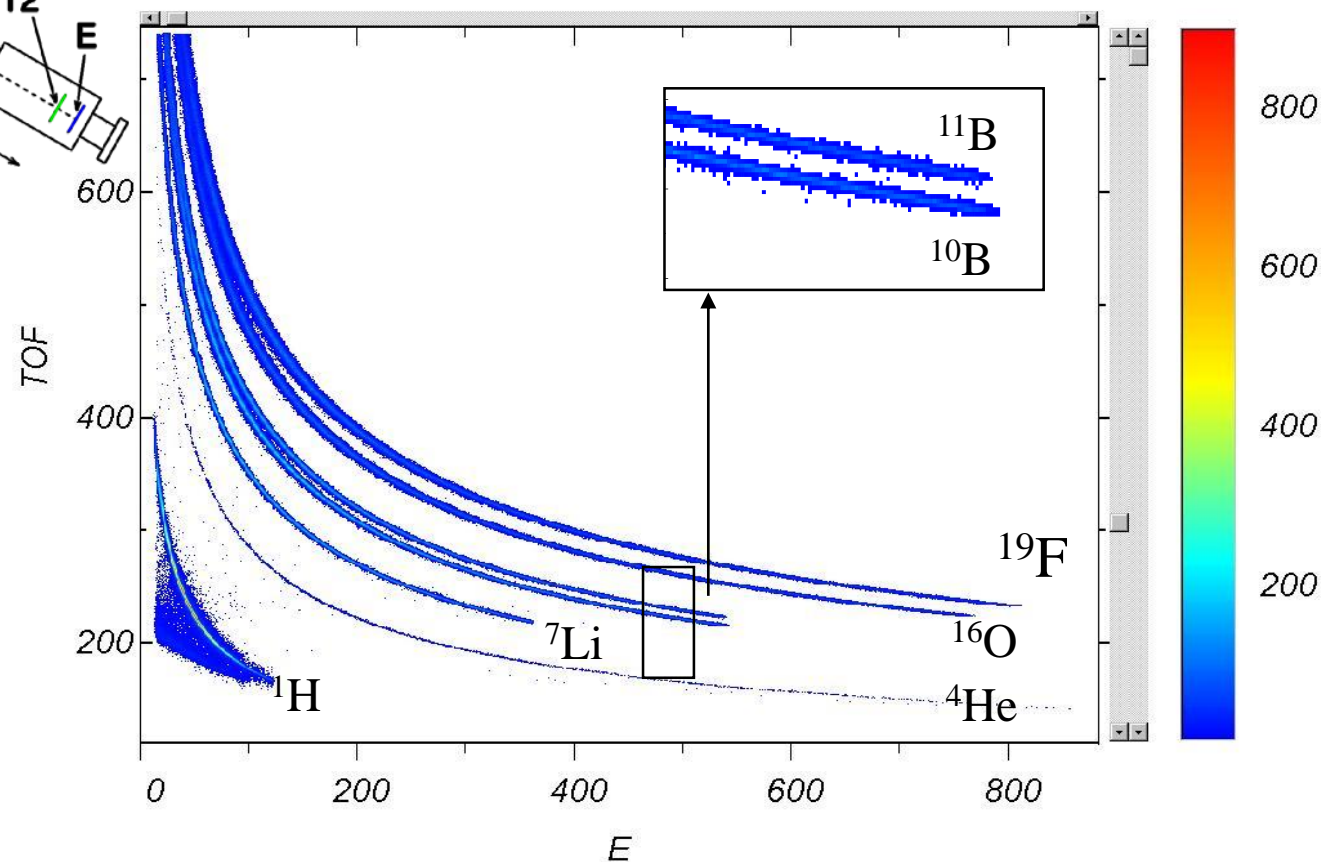
Time-of-flight ERDA

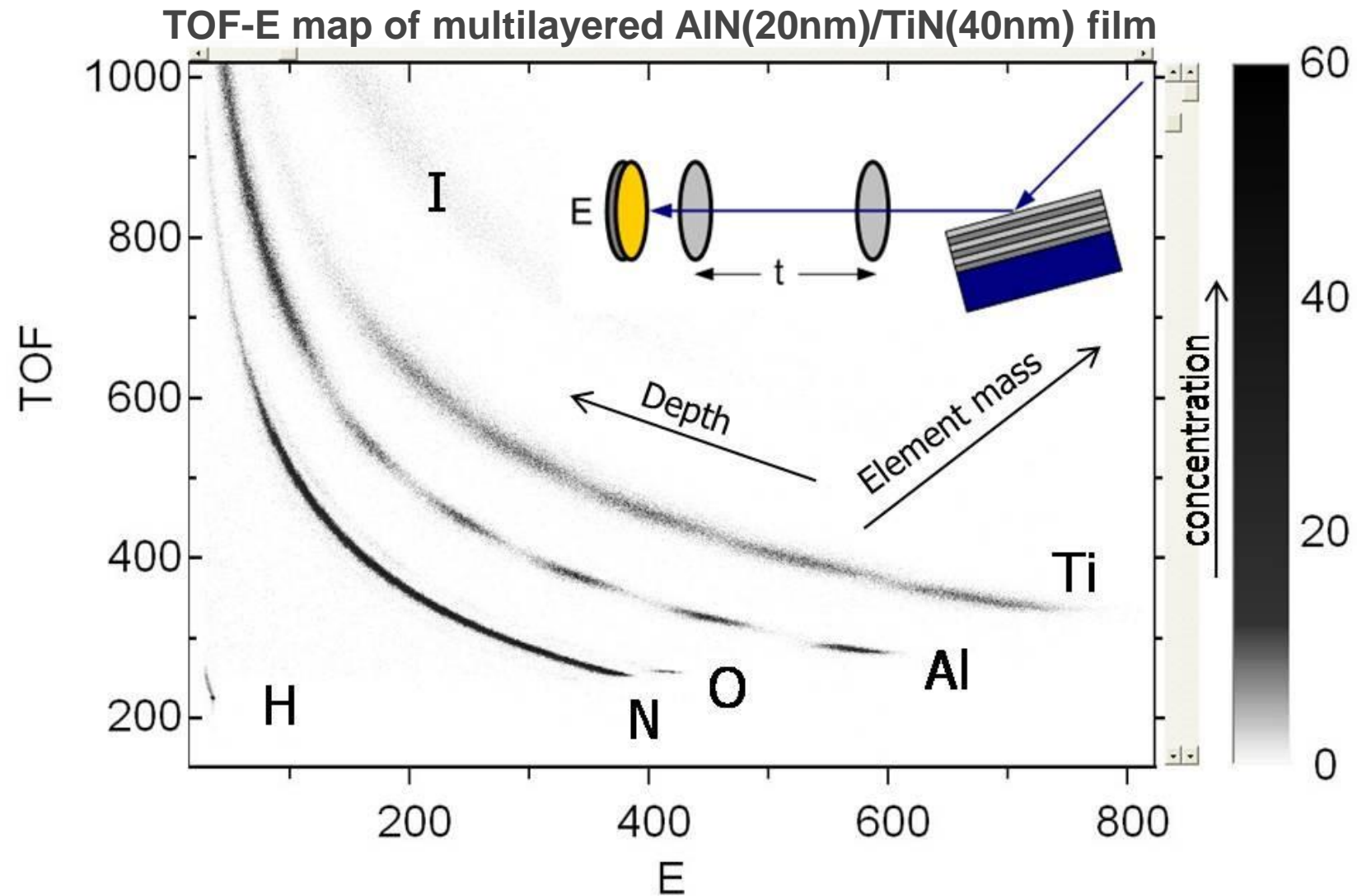


$$\Delta T = T_2 - T_1 = L(M_2/2E_r)^{1/2}$$

$$\Delta M \approx 1 \text{ up to } M=28$$

Overlapped TOF – ERDA coincidence maps: ^1H , ^4He , ^7Li , ^{10}B , ^{11}B , ^{16}O and ^{19}F ions elastically scattered from the thick Au target.





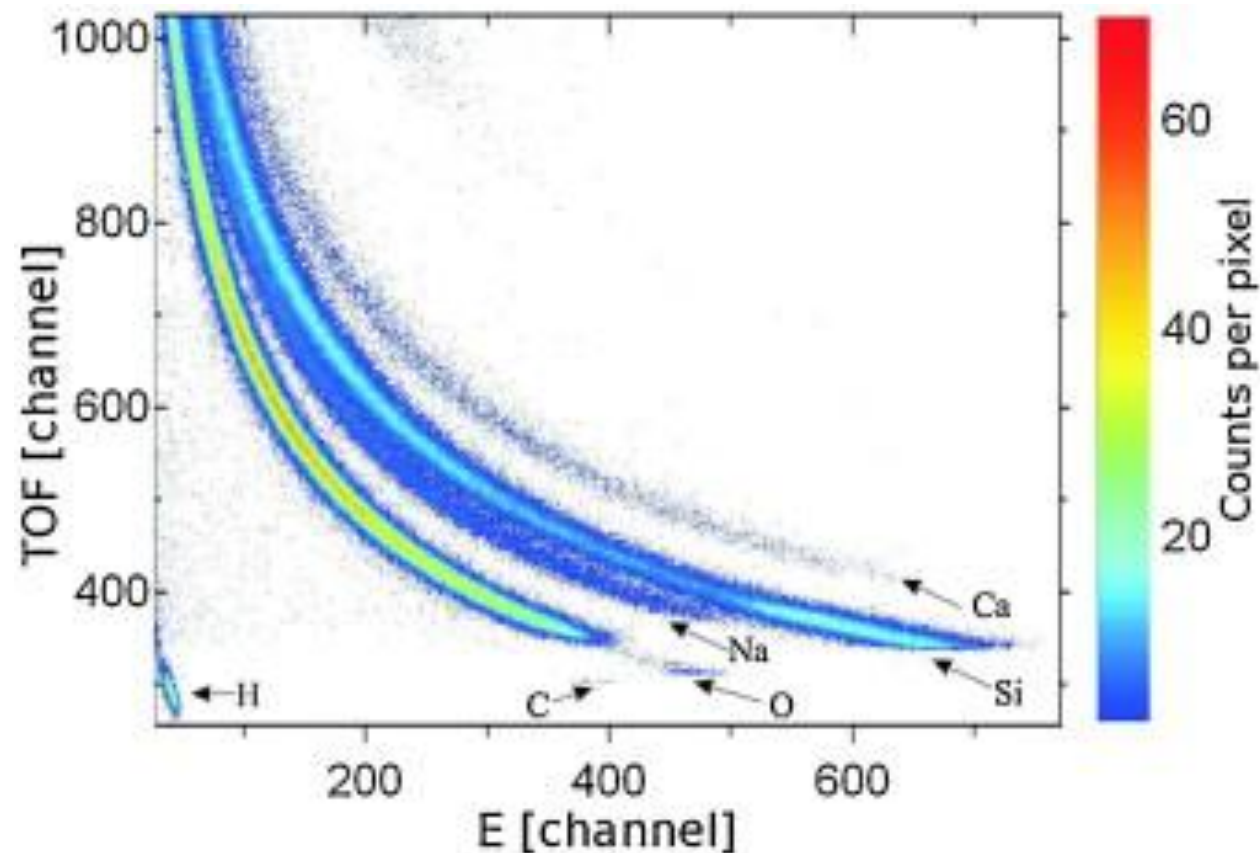


Fig. 6. TOF-ERDA coincidence map of the a-nc-Si:H sample (as deposited).

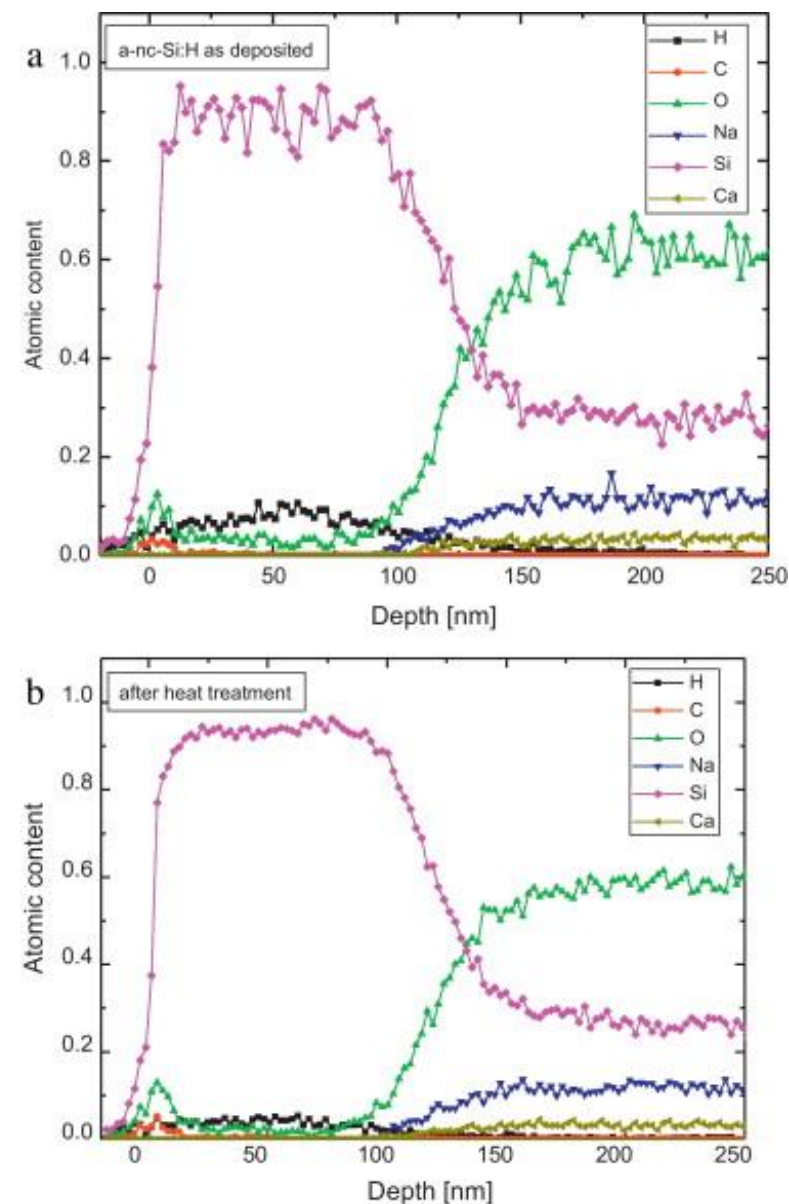
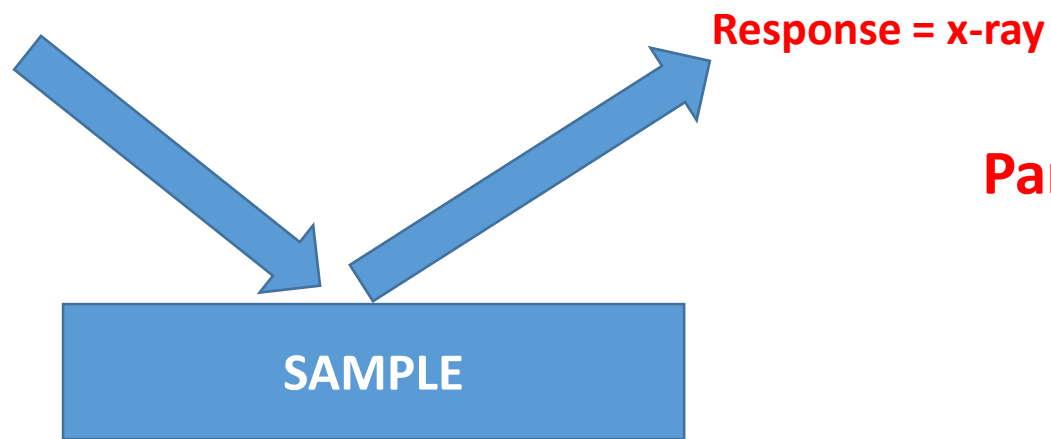


Fig. 7. Elemental analysis of the as-deposited sample (a) and the heat-treated sample (b).

Main features of ERDA

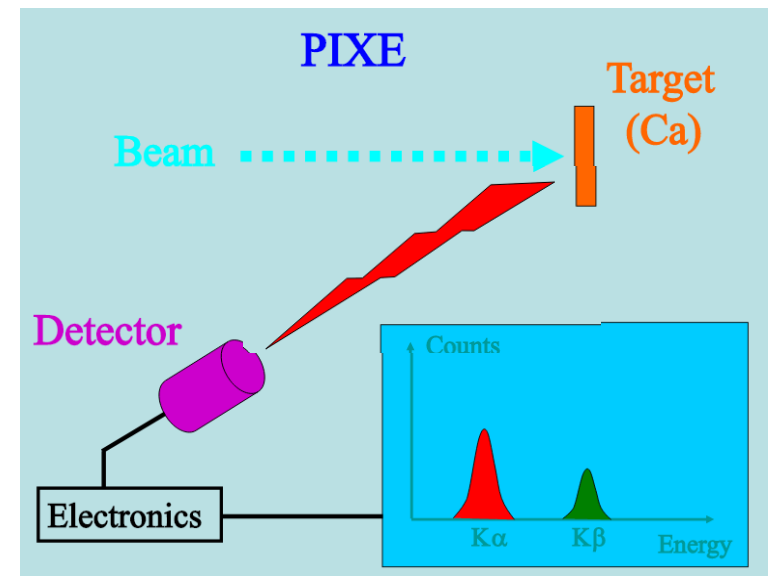
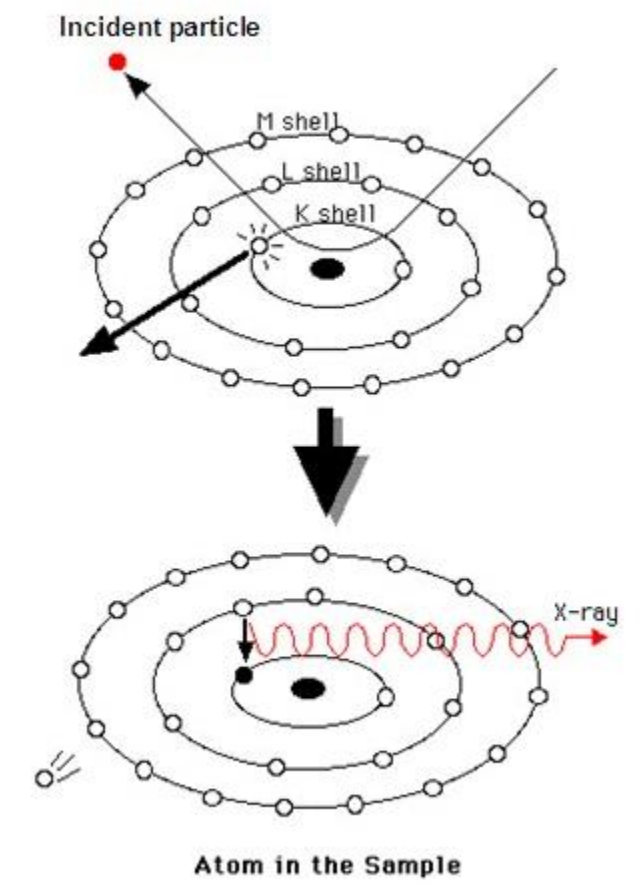
Elements	H – U (Mainly applied for hydrogen)
Standard Conditions	~100 MeV heavy ion beam (2 MeV ^4He beam for hydrogen detection) TOF, magnetic, gas ionisation detector 10 minutes per sample
Precision	Stoichiometry: 1% relative Thickness: < 5%
Sensitivity	Bulk: % to 10^{-5} , depending on Z
Depth Resolution	1 to 10 nm
Remarks	Simultaneous profiles of all elements Accessible depth range ~ $1\mu\text{m}$ Light elements detectable on heavy substrates

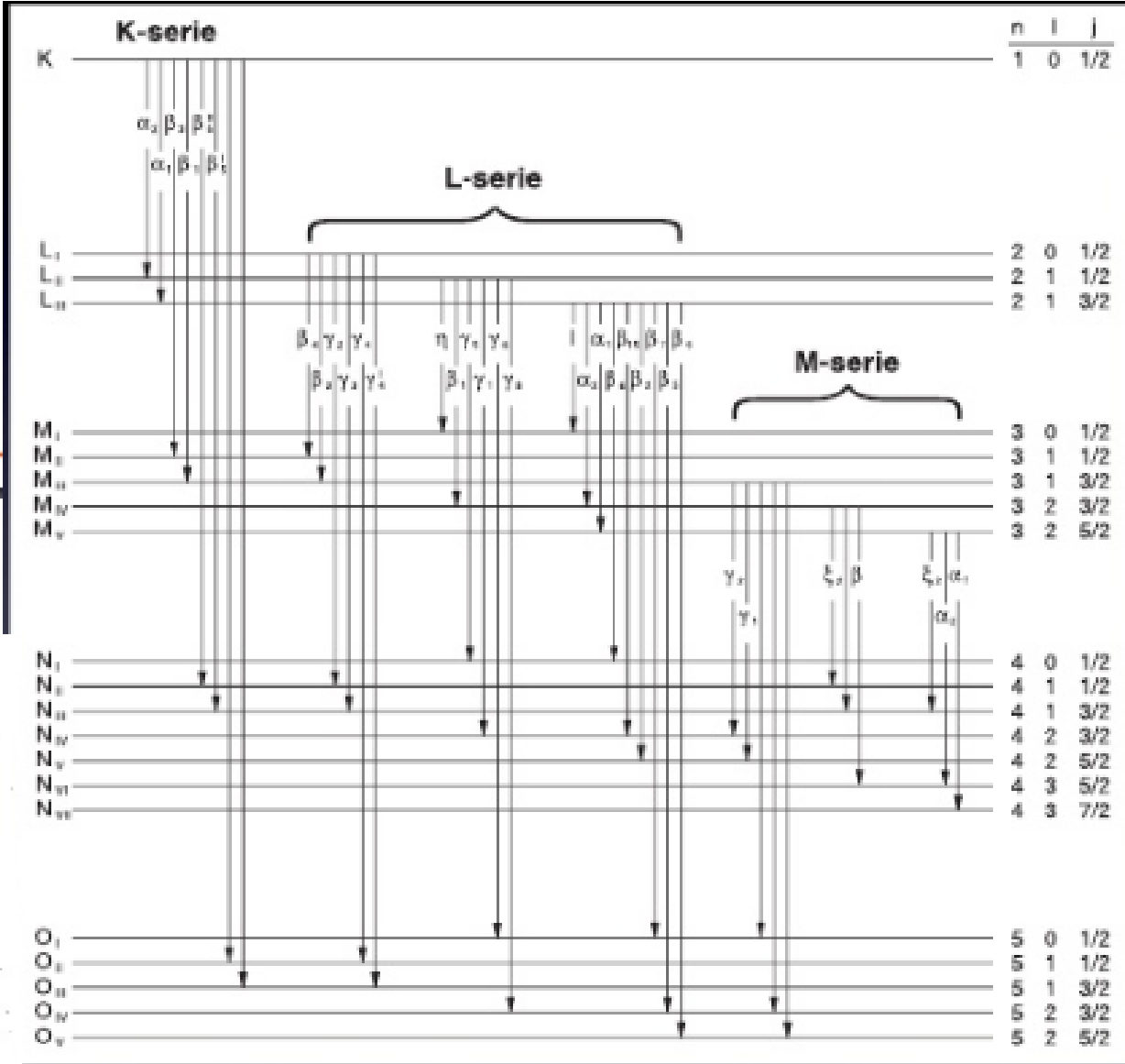
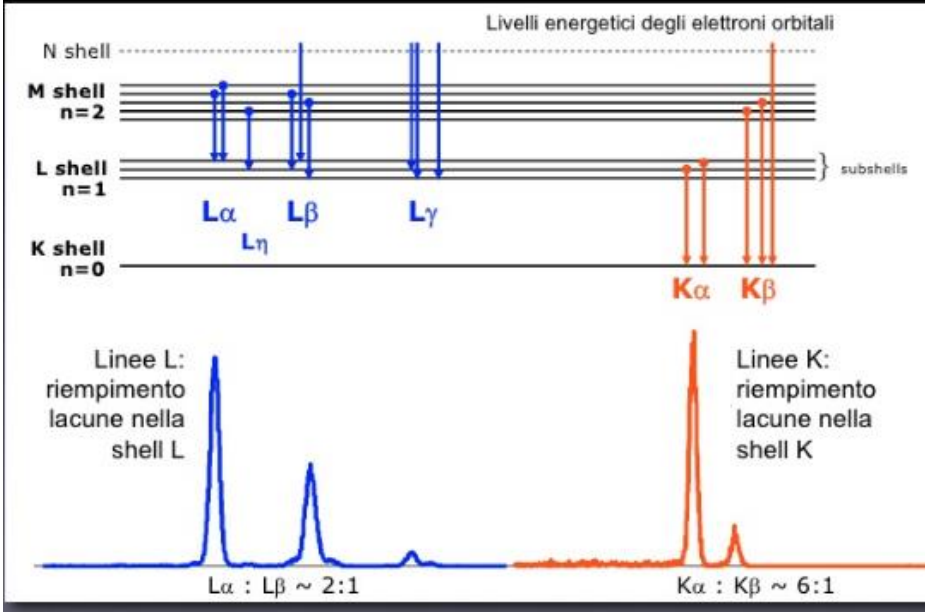
IBA-PIXE



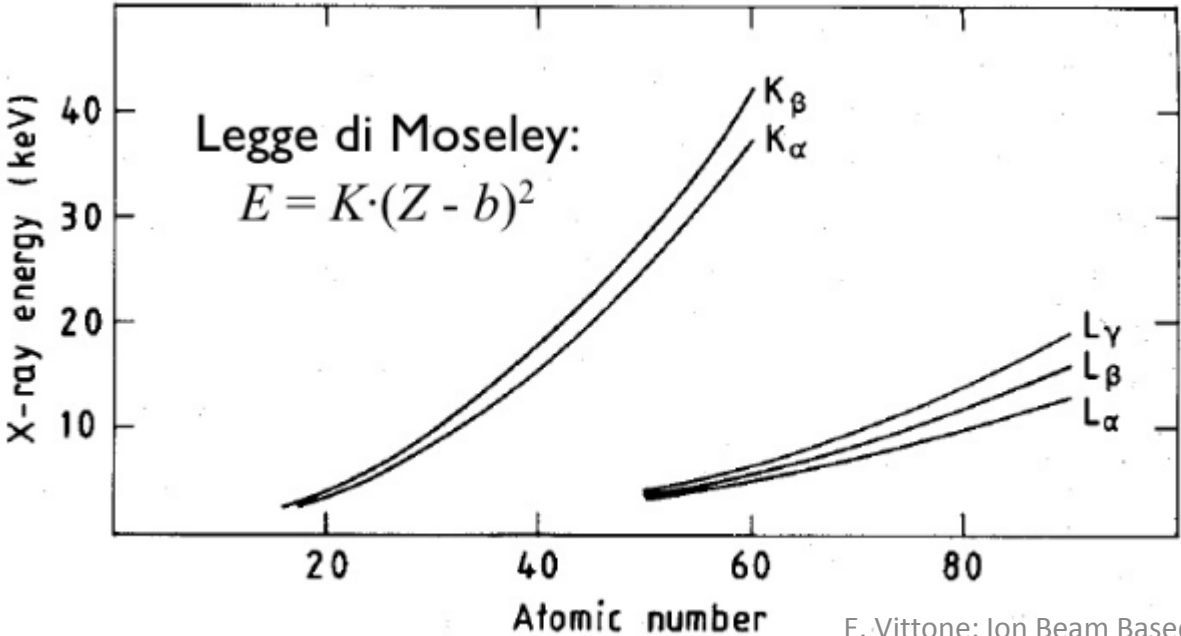
Particle (proton) induced x-ray emission

The incident ion (typically protons) eject inner shell electrons from the target atoms which results in the emission of characteristic x-rays

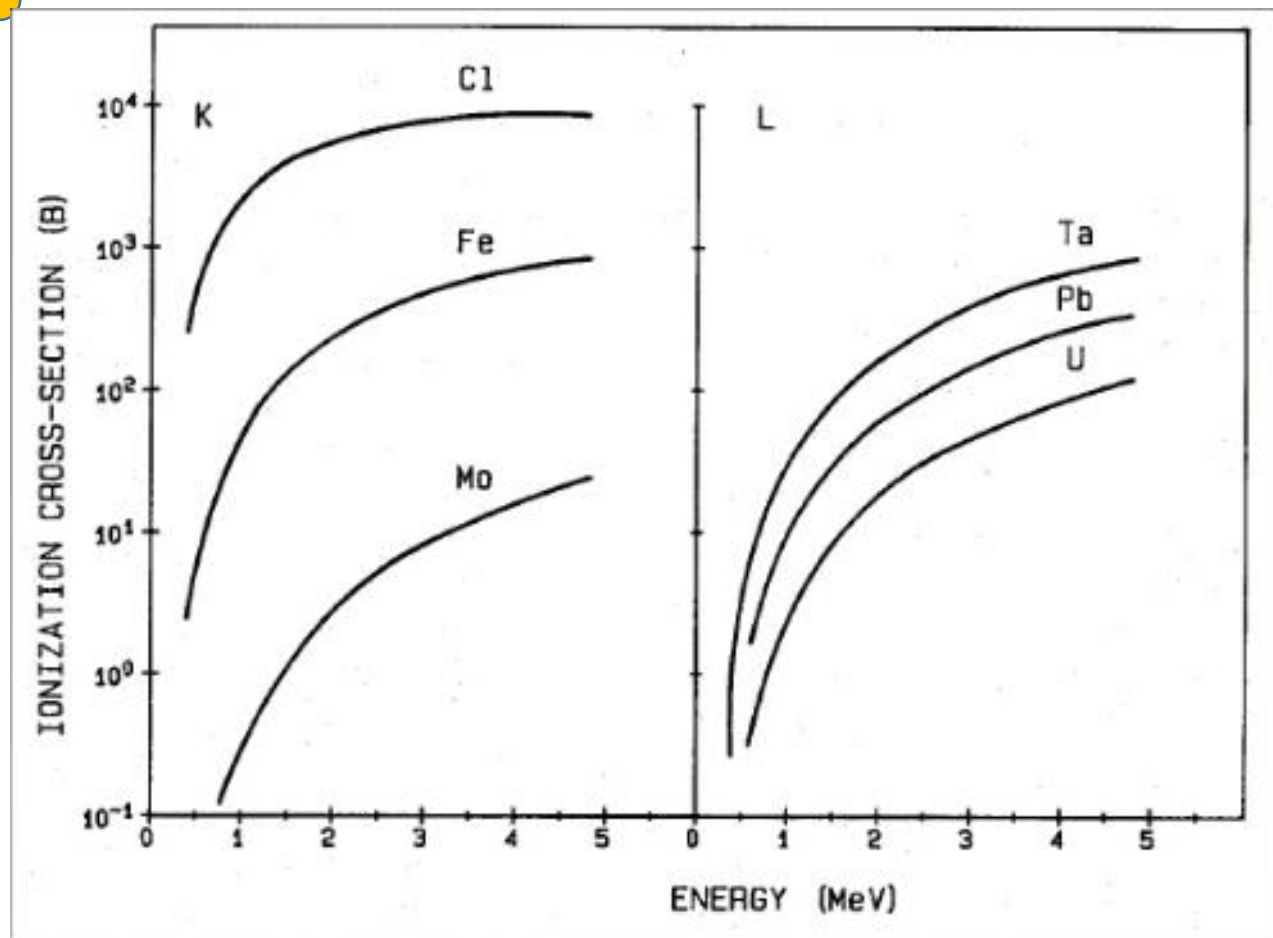




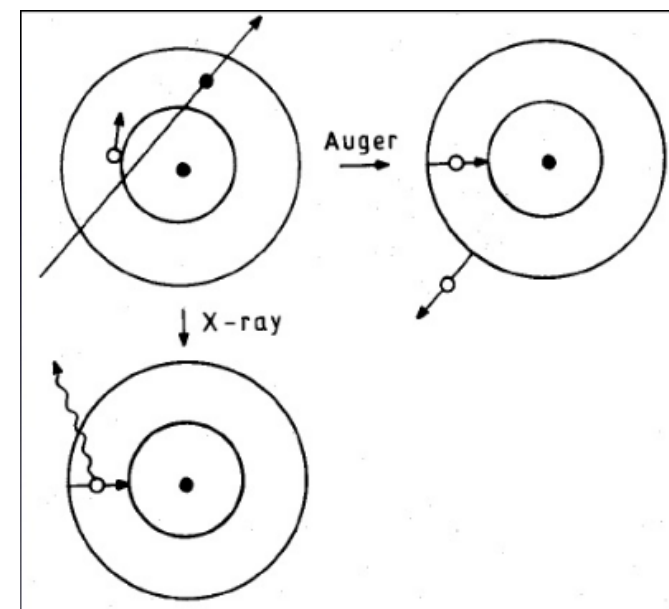
X-ray characteristic energies



Ionization cross-section



Relaxation atomic processes



X-ray production cross sections

The efficiency of X-ray production is normally measured by the x-ray production cross-section. This is the fictitious effective area that a single atom exposes to the beam assuming that each time a particle enters that area an x-ray is produced. Units are barns ($1 \text{ barn} = 10^{-24} \text{ cm}^2$).

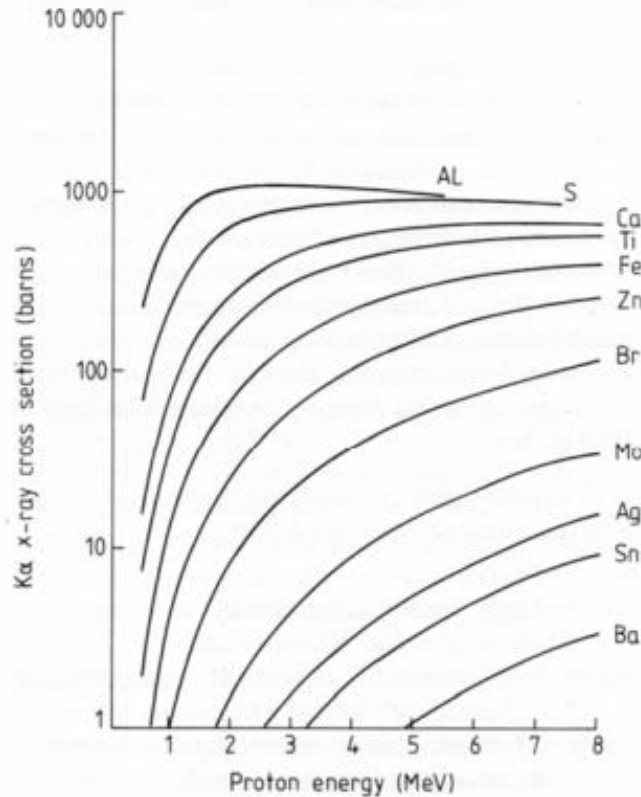


Figure 1.4 Plot of K_{α} x-ray production cross sections against incident proton energy for several common elements.

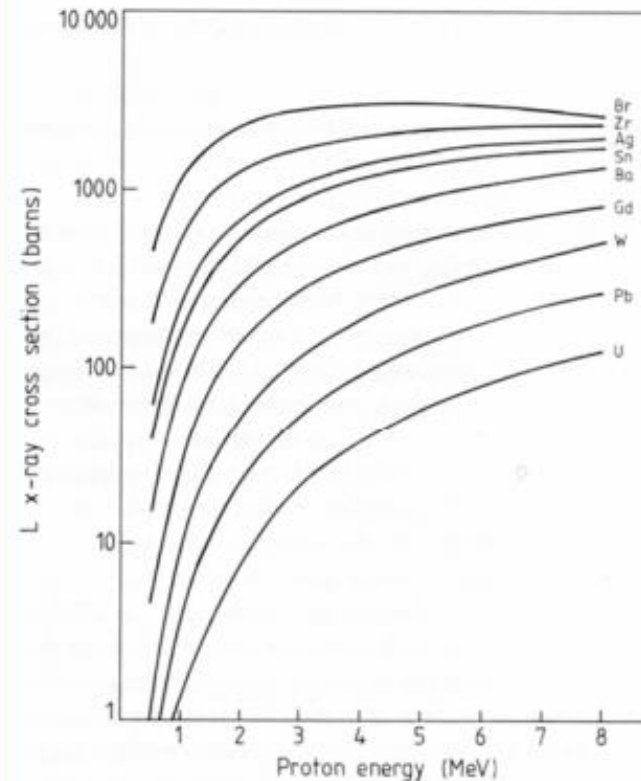
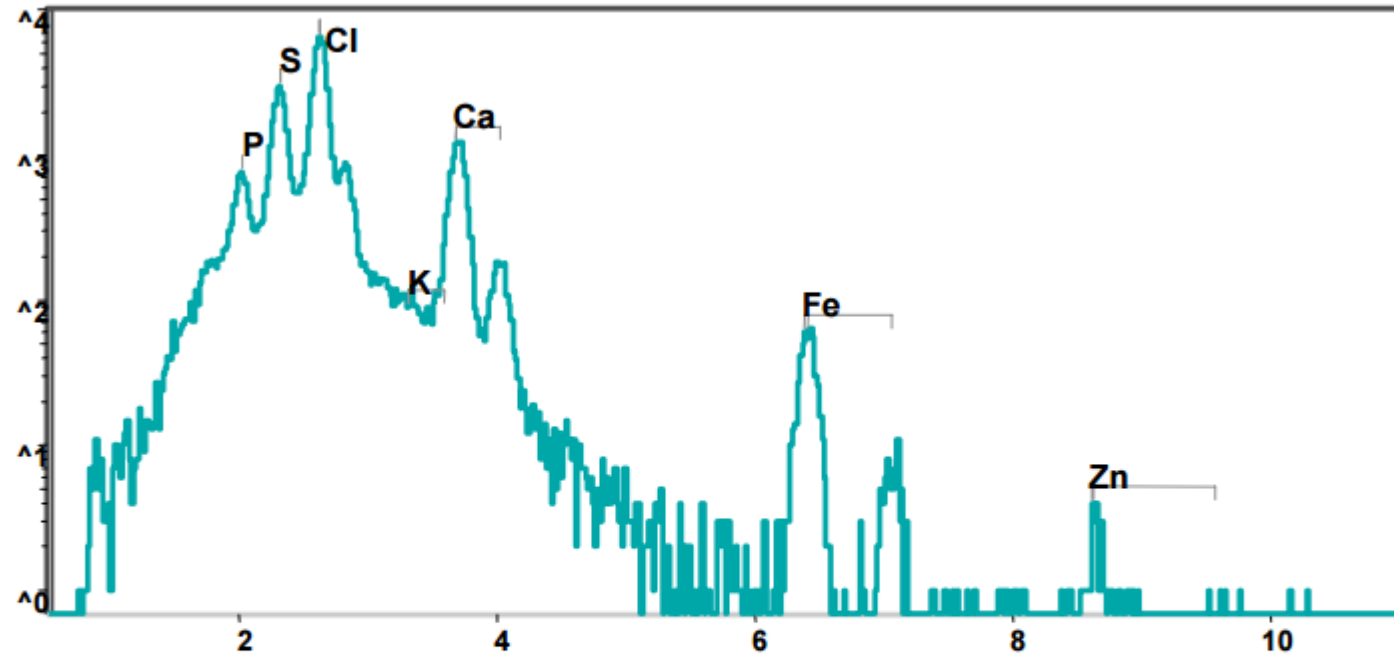


Figure 1.5 Plot of L x-ray production cross-sections against incident proton energy for several common elements.

Note that typical RBS cross sections are measured in **barns** and nuclear reaction cross sections are measured in **millibarns**.

PIXE is a very high yield technique

“Normal” PIXE spectrum



PIXE spectrum of a thin protein sample acquired using 2.5 MeV protons. This shows clear well-resolved peaks, a low energy bremsstrahlung peak with a cut-off energy of around 5.5 keV (the theoretical value for 2.5 MeV protons) and a negligible background above this.

PIXE is capable of achieving detection limits around **1 part per million (w/w)**

Using a microbeam (sampling volume $1 \mu\text{m}^3$) this corresponds to an absolute detection limit of around **10^{-18}g (1 attogram, or around 10^6 atoms)**

Total Yield of x-ray generated in a PIXE experiment

We will assume:

1. the sample is a very thin layer with N_T target atoms per cm^2 .
2. the beam has a flux of N_B protons per second (i.e. current, $I = N_B e$ ampere)
3. we are irradiating uniformly an area of $A \text{ cm}^2$ for a time t seconds (we will see that the irradiated area cancels out).

The total effective x-ray production cross section in the irradiated area is then

$$AN_T\sigma_X(E)\times 10^{-24} \text{ cm}^2 \quad \text{where } \sigma_X \text{ is the value of the x-ray cross section in barns}$$

The number of beam particles per cm^2 is $N_B t/A$, so the total number of photons created is

$$N_X = N_T N_B t \sigma_X(E) \times 10^{-24}$$

or

$$N_X = N_T I t \sigma_X(E) \times 10^{-24} / e$$

or

$$N_X = N_T Q \sigma_X(E) \times 10^{-24} / e$$

Where Q is the total beam charge in C and e is the electronic charge, $1.6 \times 10^{-19} \text{ C}$

Assuming that the X-rays are emitted isotropically and that the detector has a solid angle of Ω sr and an intrinsic efficiency of $\varepsilon(E_x)$, the total number of detected X-rays is

$$N_X = N_T Q \sigma_X(E) \Omega \varepsilon(E_X) \times 10^{-19} / 4\pi e$$

This can be written in terms of the areal density of the target atoms, $m \mu\text{g cm}^{-2}$ as follows:

$$N_X = m Q Y(E) \Omega \varepsilon(E_x)$$

where

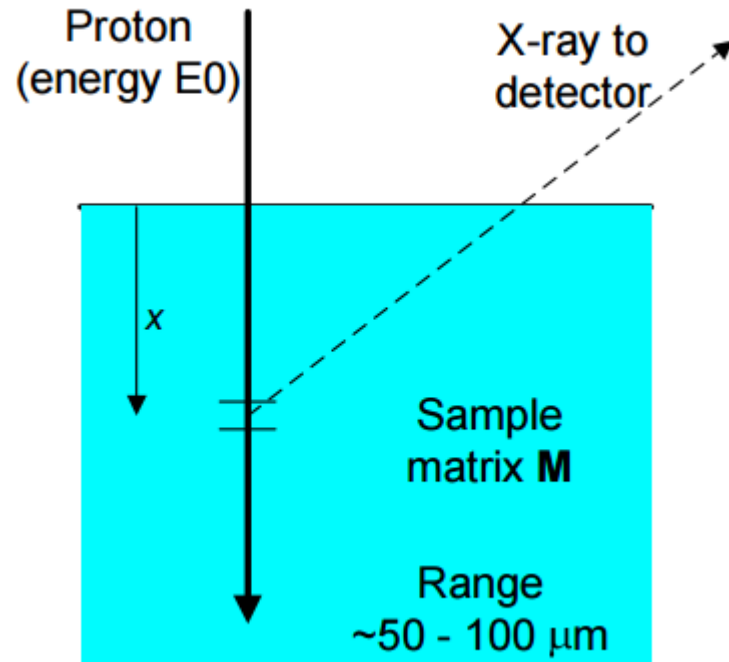
$$Y(E) = \frac{\sigma_X(E) \times 10^{-24}}{4\pi e A m_p} \approx 3 \times 10^5 \frac{\sigma_X(E)}{A} \text{ counts}/\mu\text{C}/\mu\text{gcm}^{-2}/\text{sr}$$

where $A m_p$ is the mass of the target atom.

Y is the thin target PIXE yield. This is a function of the Z and A of the target atom, the type and energy of the incident ion and the measured X-ray transition.

Typical values (e.g. for Ca Ka X-rays induced by 3MeV protons) are $\sim 10^6$ cts/ $\mu\text{C}/\mu\text{gcm}^{-2}/\text{sr}$

Absorption of the emitted x-ray



At depth x :

- Proton energy, $E(x)$ depends on E_0 , x and stopping power, S , of M
- X-ray production cross section, σ , depends on $E(x)$ and Z
- Absorption of emitted x-ray depends on the X-ray mass absorption coefficient, μ , of M , the energy of the xray and the angle of the detector

$$dN_Z = KQc_Z\sigma_x(Z, E)\Omega\varepsilon(E_Z)\exp\left(-\mu(M, E_Z)\frac{x}{\cos\theta}\right)dx$$

where c_Z is now the mass fraction of Z in the matrix

Software Packages

AXIL, GEOPIXE II, PIXYKLM, GUPIX/Dan32

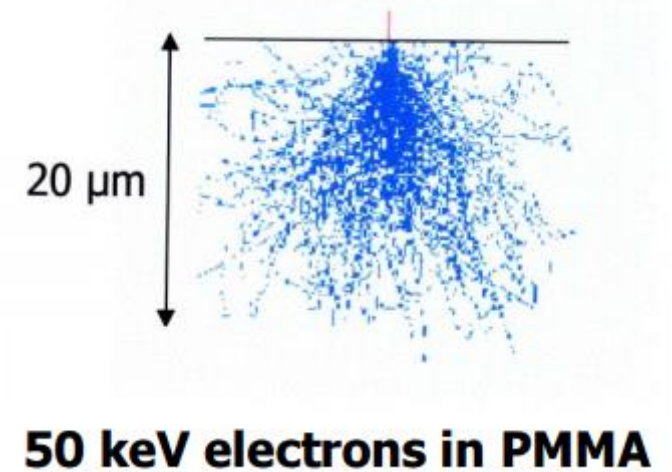
- Rapid, sensitive and non - destructive analyses
- Quantitative analysis; LOW DETECTION LIMIT
- Minimum detectable x-ray energy: 1 keV → All the elements with $Z > 11$ can be simultaneously detected
- PIXE is the analogon to Energy Dispersive X-ray analysis (EDX) with electron microprobe.
- Trace element analysis using PIXE has a detection limit orders of magnitude lower than can be attainable by x-ray spectrometry techniques using electron excitation.
- Under favorable conditions, a detection limit ~1 ppm for thin foils and ~10 ppm for thick samples can be achieved.

<http://indico.ictp.it/event/a05196/session/16/contribution/8/material/0/0.pdf>

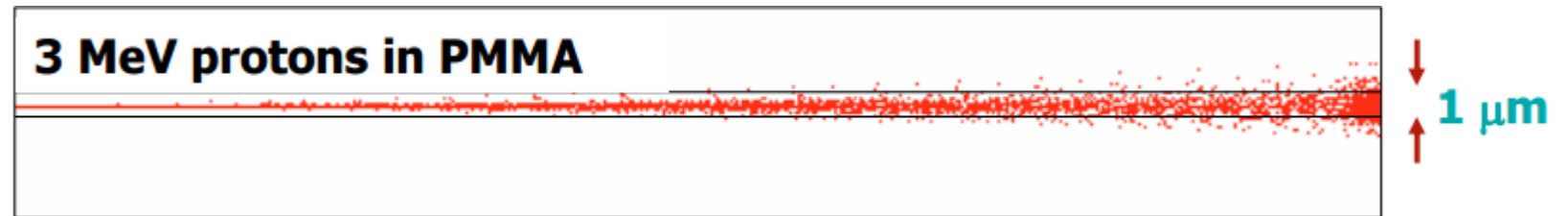
Sources of background:

Primary proton bremsstrahlung

High mass of protons means that they have very small deflection at each electron collision. This means that primary bremsstrahlung is essentially absent.



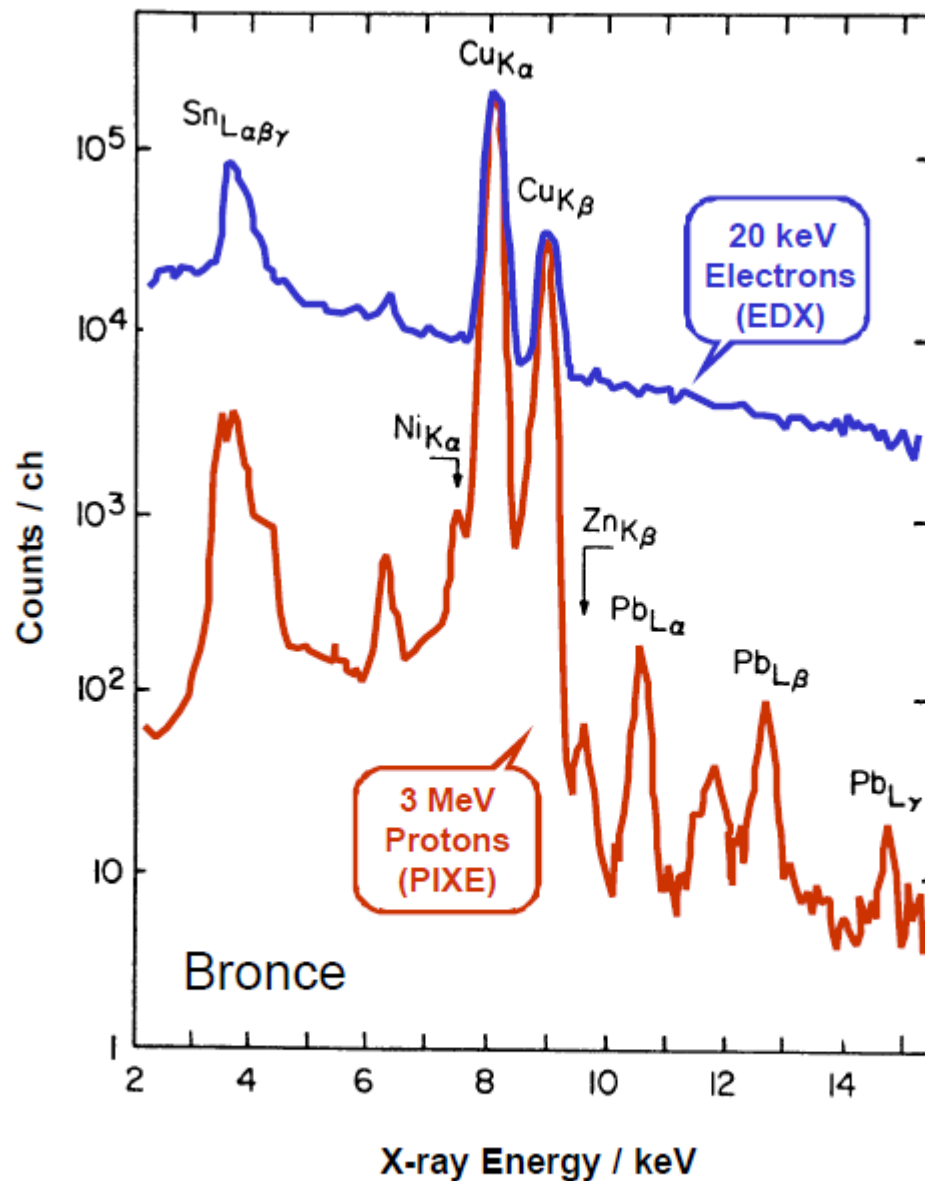
3 MeV protons in PMMA



Secondary electron bremsstrahlung (SEB)

- The electron removed by ionisation may either collide with nearby electrons and eventually stop, or execute an orbit returning to its parent atom (synchrotron radiation). In each case bremsstrahlung is emitted.
- The maximum energy that can be transferred to an electron in a proton-electron collision is or about 6.5 keV for 3MeV protons. This means that SEB only affects the lower energy part of the spectrum.
- SEB is a secondary process! The number of secondary electrons created is orders of magnitude lower than the number of primary particles

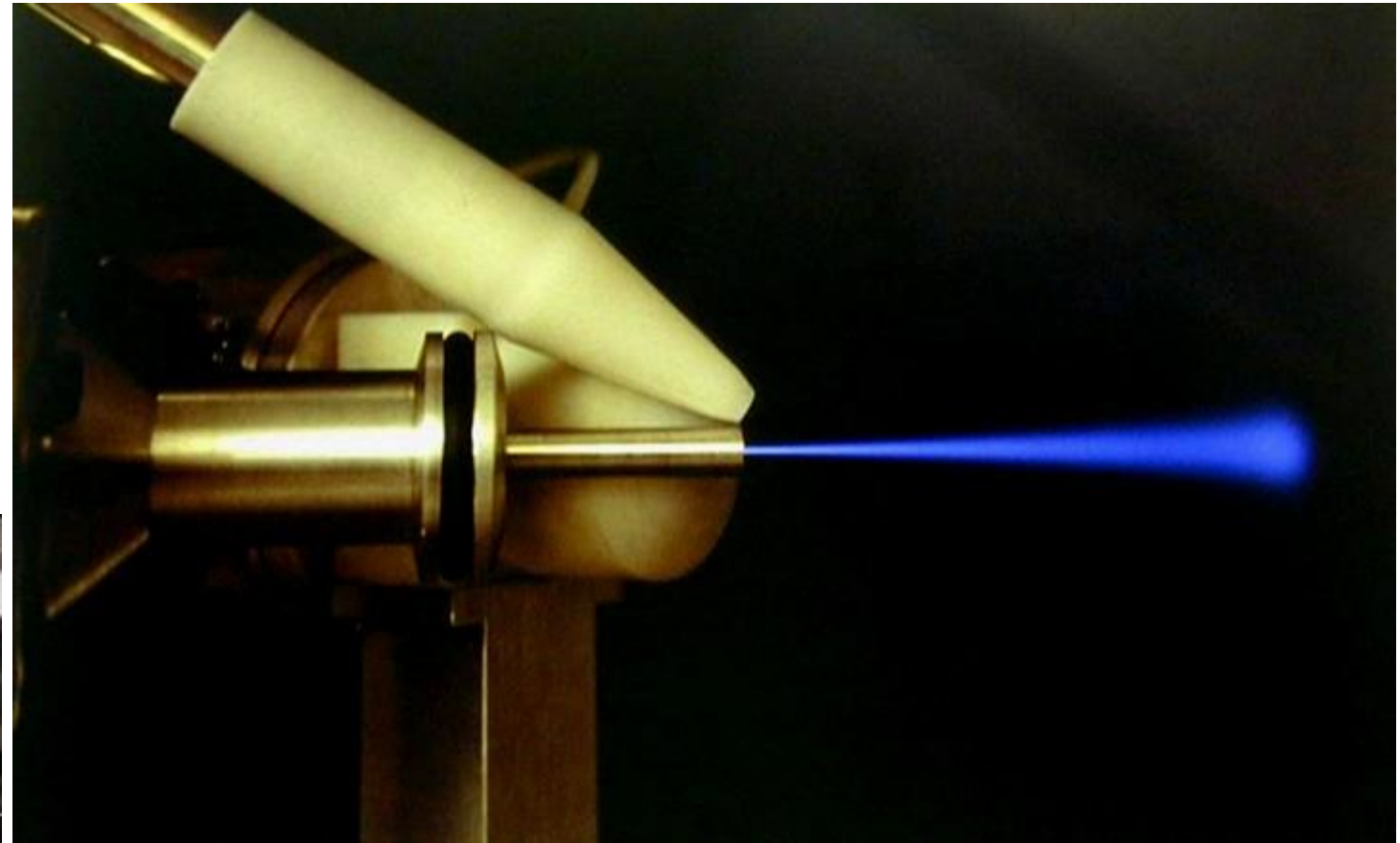
Very low background (no primary bremsstrahlung), so ppm detection limits



IBA-PIXE

External Beam

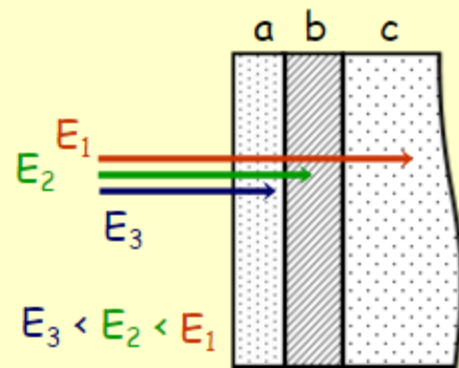
Application in cultural heritage
Non vacuum-compatible objects
(e.g. biological samples)



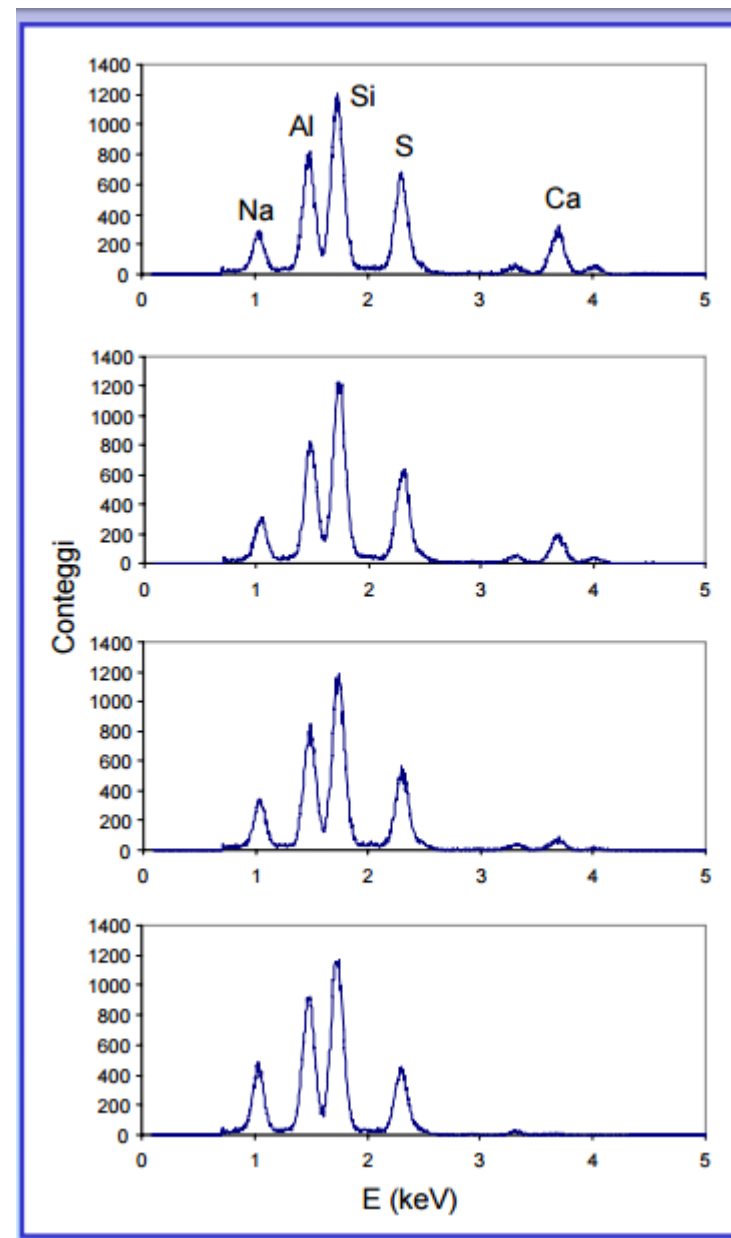
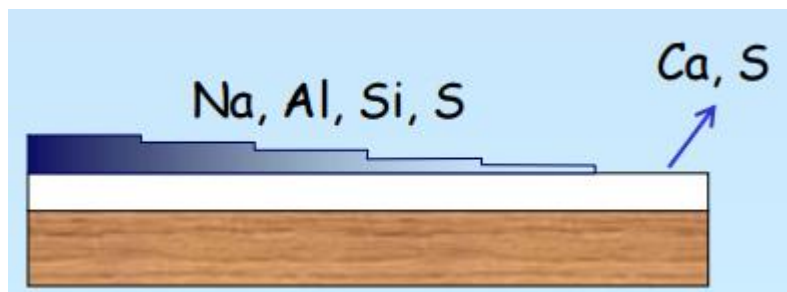
<http://www.le.infn.it/ifaef/PDF/N.Grassi-UltimaVersione.pdf>

<http://slideplayer.com/slide/10496042/>

Measurements on the same spot
with different beam energies



Wooden tablet with a plaster base and Painted
with layers of different thickness of lapis lazuli



Decreasing Beam Energy----->

Elements	Al - U
Standard Conditions	3 MeV proton beam Si(Li), Ge detector 10 minutes per sample
Precision	Stoichiometry: 5% relative Generally used for trace element analysis Absolute concentrations mainly by calibration standards
Sensitivity	1 to 100 ppm, depending on Z and matrix
Depth Resolution	No depth information
Remarks	Probed depth is tens of μm Often used with raster imaging (proton microprobe)

Summary of PIXE

- High yield (rapid!) trace element analysis
- Detects all elements simultaneously
 - Element range set by detector response: typically Na – U
- Very low background (no primary bremsstrahlung), so ppm detection limits
- Yield can be calculated from fundamental physics, so you can get good accuracy with a minimal dependence on standard reference materials.

Technique	Measured signal	Spatial Resolution (μm)	Depth resolution (μm)	Detectable elements (Z)	Detection sensitivity (wppm)	Quantitativity (%)
PIXE	X-rays	0.3	5	>11	0.1	5
RBS	Backscattered ions	0.5	0.02	>2	1	3
NRA	Charged particle reaction products	1	0.005	All low Z	0.01	3
ERDA	Forward scattered sample ions	>1	0.005	<15	500	3
SIMS	Sample ions	0.05	0.005	All	0.001-10	50
AES	Auger electrons	0.1	0.001	>2	10000	50
XPS	Photoelectrons	1000	0.002	>2	1000	50
EDS	X-rays	0.5	1	>6	100	1
XRF	X-rays	3	5	>11	1	5

C. Jeynes, R.P. Webb, A. Lohstroh

Ion Beam Analysis: A century of exploiting the electronic and nuclear structure of the atom for materials characterization

<https://www.surrey.ac.uk/ati/ibc/files/IBAchapter-Final.pdf>

P. Mandò,

Applications of nuclear techniques to Art & Archaeology

<http://slideplayer.com/slide/10496042/>

J. Grime,

Broadbeam PIXE – Concepts and Applications

<http://indico.ictp.it/event/a05196/session/16/contribution/8/material/0/0.pdf>

M. Döbeli

Material Analysis

<http://cas.web.cern.ch/cas/Pruhonice/PDF/Doebeli.pdf>

M. Mayer

Rutherford Backscattering Spectrometry (RBS)

http://users.ictp.it/~pub_off/lectures/Ins022/Mayer_1/Mayer_1.pdf

IAEA TECDOC 1190

Instrumentation for PIXE and RBS

<http://www-pub.iaea.org/books/iaeabooks/5966/Instrumentation-for-PIXE-and-RBS>

M. Chiari

La tecnica RBS

www.slideshare.net/max0068/chiari-lezione-su-rutherford-backscattering-spectrometry-rsb-2012

M. Chiari

La tecnica PIXE

<https://www.slideshare.net/max0068/chiari-lezione-su-particle-induced-xray-emission-pixe-2012>

Y. Wang, M. Nastasi

Handbook of Modern Ion Beam Materials Analysis

Material Research Society, 2° edition, 2009, www.mrs.org